Received: 20 July 2017 | Revised: 22 August 2017 | Accepted: 1 September 2017

DOI: 10.1002/pld3.14

ORIGINAL RESEARCH

ALUMINUM RESISTANCE TRANSCRIPTION FACTOR 1 (*ART1*) contributes to natural variation in aluminum resistance in diverse genetic backgrounds of rice (*O. sativa*)

Juan D. Arbelaez[1]* | Lyza G. Maron[1]* | Timothy O. Jobe[1,2] | Miguel A. Piñeros[3] | Adam N. Famoso[1] | Ana Rita Rebelo[1] | Namrata Singh[1] | Qiyue Ma[2] | Zhangjun Fei[2] | Leon V. Kochian[3] | Susan R. McCouch[1]

[1]Plant Breeding and Genetics Section, School of Integrative Plant Science, Cornell University, Ithaca, NY, USA

[2]Boyce Thompson Institute, Cornell University, Ithaca, NY, USA

[3]Robert W. Holley Center for Agriculture and Health, USDA-ARS, Cornell University, Ithaca, NY, USA

Correspondence
Susan R. McCouch, Plant Breeding and Genetics Section, School of Integrative Plant Science, Cornell University, Ithaca, NY, USA.
Email: srm4@cornell.edu

Present addresses
Juan D. Arbelaez, Plant Breeding, International Rice Research Institute, Los Baños, Philippines.
Timothy O. Jobe, Botanical Institute, University of Cologne, Cologne, Germany.
Adam N. Famoso, LSU AgCenter, H. Rouse Caffey Rice Research Station, Rayne, LA, USA.
Ana Rita Rebelo, Boyce Thompson Institute, Cornell University, Ithaca, NY, USA.
Leon V. Kochian, Global Institute for Food Security, University of Saskatchewan, Saskatoon, SK, Canada

Funding information
This work was supported by a grant from USDA-NIFA, award # 2013-67013-21379; NSF-PGRP award #1026555; a PhD fellowship for JDA from the Monsanto Beachell-Bourlag International Scholars Program.

Abstract

Transcription factors (TFs) regulate the expression of other genes to indirectly mediate stress resistance mechanisms. Therefore, when studying TF-mediated stress resistance, it is important to understand how TFs interact with genes in the genetic background. Here, we fine-mapped the aluminum (Al) resistance QTL *Alt12.1* to a 44-kb region containing six genes. Among them is *ART1*, which encodes a C2H2-type zinc finger TF required for Al resistance in rice. The mapping parents, Al-resistant cv Azucena (*tropical japonica*) and Al-sensitive cv IR64 (*indica*), have extensive sequence polymorphism within the *ART1* coding region, but similar *ART*1 expression levels. Using reciprocal near-isogenic lines (NILs) we examined how allele-swapping the *Alt12.1* locus would affect plant responses to Al. Analysis of global transcriptional responses to Al stress in roots of the NILs alongside their recurrent parents demonstrated that the presence of the *Alt12.1* from Al-resistant Azucena led to greater changes in gene expression in response to Al when compared to the *Alt12.1* from IR64 in both genetic backgrounds. The presence of the ART1 allele from the opposite parent affected the expression of several genes not previously implicated in rice Al tolerance. We highlight examples where putatively functional variation in *cis*-regulatory regions of ART1-regulated genes interacts with ART1 to determine gene expression in response to Al. This ART1–promoter interaction may be associated with transgressive variation for Al resistance in the Azucena × IR64 population. These results illustrate how ART1 interacts with the genetic background to contribute to quantitative phenotypic variation in rice Al resistance.

KEYWORDS
abiotic stress, acid soils, aluminum, QTL mapping, rice, transcriptional regulation

*Contributed equally.

This manuscript was previously deposited as a preprint at doi: https://www.biorxiv.org/content/early/2017/09/01/137281

1 | INTRODUCTION

Plants achieve abiotic stress resistance through diverse mechanisms that evolved through both natural and artificial selection. The characterization of quantitative trait loci (QTL) and their underlying genes has led to insights about the genetic architecture and the biological mechanisms of resistance to several abiotic stresses. Two major classes of genes predominate as determinants of stress resistance: membrane transporters and transcription factors (TFs) (Mickelbart, Hasegawa, & Bailey-Serres, 2015). The reprogramming of gene expression through transcriptional regulation, mediated by TFs, is a finely orchestrated and tightly regulated process, and is one of the hallmarks of plant response to stress (Vaahtera & Brosché, 2011). To achieve specificity in the transcriptional response, a TF must activate only target genes involved in adaptation to a particular stress or combination of stresses (Vaahtera & Brosché, 2011). TFs are activated through posttranslational modification and nuclear import and/or may be transcriptionally activated by other TFs. Genetic variation in the TF loci, or in any element along the regulatory chain, can contribute to phenotypic variation in plant stress resistance. Understanding the quantitative nature of TF-mediated stress resistance in plants is essential when predicting the impact of introducing alleles into a new genetic background in the context of plant breeding and crop improvement.

Aluminum toxicity severely limits plant growth on acidic soils (pH <5). Under these conditions, the rhizotoxic Al species Al^{3+} is solubilized, inhibiting root growth and function (Kochian, Piñeros, Liu, & Magalhaes, 2015), and leaving plants more vulnerable to drought and mineral nutrient deficiencies. Approximately 30% of the earth's land area consists of highly acid soils, and as much as 50% of all potentially arable lands are acidic (von Uexküll & Mutert, 1995). As vast areas of acid soils in the tropics and subtropics are critical food-producing regions, Al toxicity constitutes a food security threat exceeded only by drought among the abiotic limitations to crop production.

Rice (*Oryza sativa* L.) is the most Al-resistant species among the small grain cereals (Foy, 1988; Ma et al., 2002). A comparative cross-species study in hydroponics showed that rice is two- to six-fold more resistant than maize, wheat, and sorghum (Famoso et al., 2010). This high level of resistance is likely achieved by the pyramiding of multiple mechanisms conferred by multiple genes, a hypothesis supported by results from both genome-wide association (GWAS) and QTL studies (Famoso et al., 2011). Mapping of Al resistance QTL in a rice recombinant inbred line (RIL) population derived from a cross between Al-resistant Azucena (*O. sativa* L., *tropical japonica*) and Al-sensitive IR64 (*O. sativa* L., *indica*) cultivars identified four genomic regions associated with Al resistance, on chromosomes 1, 2, 9, and 12 (Famoso et al., 2011; Spindel et al., 2013). The QTL *Alt12.1* on chromosome 12, which explains a large proportion (>19%) of the variation in Al resistance, encompasses a genomic region that includes the gene *ALUMINUM RESISTANCE TRANSCRIPTION FACTOR 1* (*ART1*), encoding a C2H2-type zinc finger transcription factor (Yamaji et al., 2009). The *art1* mutant, producing a truncated version of the ART1 protein, is sensitive to Al stress.

A total of 32 genes were up-regulated in response to Al in the wild type but were not up-regulated in the *art1* mutant (Yamaji et al., 2009). Some of these genes have been shown to play a role in rice Al resistance. These "ART1-regulated genes" have received this denomination because they are mis-regulated in the *art1* mutant; in other words, their expression is up-regulated by Al stress in the wild type, but not in the mutant (Yamaji et al., 2009). It is worth noting that direct binding of the ART1 protein to upstream regulatory regions has so far been experimentally demonstrated only for *STAR1* (Tsutsui, Yamaji, & Ma, 2011) and *OsFRDL4* (Yokosho, Yamaji, Kashino-Fujii, & Ma, 2016).

The genetic architecture of rice Al resistance is complex and quantitative in nature (Famoso et al., 2011). In the present study, we describe how natural variation in the *ART1* locus affects transcriptional responses to Al stress in two distinct genetic backgrounds of rice. We fine-mapped the Al resistance QTL *Alt12.1* to a small region surrounding *ART1* and used reciprocal near-isogenic lines (NILs) to examine the effect of two different *ART1* alleles in *japonica* (Al-resistant Azucena) and *indica* (Al-sensitive IR64) genetic backgrounds. Analysis of the global transcriptional response to Al stress in roots of the reciprocal NILs demonstrated that the presence of the *Alt12.1* locus from Al-resistant Azucena induced greater changes in gene expression in response to Al stress when compared to the *Alt12.1* locus from IR64 in both genetic backgrounds. These changes were observed in a number of genes in addition to those previously reported as ART1-regulated. Moreover, our data suggest that the changes in gene expression pattern in response to the ART1 allele swapping may be background-specific, suggesting that natural variation in *cis*-regulatory regions also plays a role in determining gene expression responses to Al. These results demonstrate the importance of genetic background in determining the phenotypic impact of a major Al resistance gene.

2 | RESULTS

2.1 | Development and evaluation of reciprocal near-isogenic lines (NILs) for the Al resistance QTL *Alt12.1*

We developed reciprocal near-isogenic lines (NILs) in the Azucena (Al-resistant) and IR64 (Al-sensitive) genetic backgrounds to examine how allele swapping at the *Alt12.1* QTL would affect plant responses to Al (Figure 1). The chromosomal region harboring *Alt12.1* from the Al-resistant parent Azucena was introduced into IR64 via backcrossing, and vice versa (Appendix S1). Phenotypically, the aboveground parts of $AZU_{[IR6412.1]}$ and $IR64_{[AZU12.1]}$ plants closely resemble their respective recurrent parents when grown under greenhouse conditions (Figure 1a). The NIL $AZU_{[IR6412.1]}$ contains a 3.92-Mb introgression from IR64 encompassing *Alt12.1* in the Azucena background, while the reciprocal NIL $IR64_{[AZU12.1]}$ carries a 2.36-Mb Azucena

introgression spanning the *Alt12.1* locus in the IR64 genetic background. Both NILs carry a single donor introgression across the target region, while over 99% of their genomes are identical to the recipient background (Figure 1c; Table S2). When evaluated for Al resistance based on relative root growth (RRG) in hydroponics, the NIL $AZU_{[IR6412.1]}$ was significantly ($p < .05$) less Al-resistant than its recurrent parent Azucena. Conversely, $IR64_{[AZU12.1]}$ was significantly ($p < .05$) more Al-resistant than its recurrent parent, IR64 (Figure 1b–d, Table S2). These results validate the effect of the *Alt12.1* QTL on Al resistance in both genetic backgrounds.

2.2 | Fine-mapping of the *Alt12.1* QTL

The *Alt12.1* locus was fine-mapped using a substitution mapping approach (Appendix S2) to a 0.2 cM region (44.7 kb; chromosome 12: 3,578,363 - 3,623,299 bp), between markers *K_3.57* and *indel_3.62* (Figure 2a, Fig. S1, Table S1). According to the rice MSUv.7 genome assembly (Kawahara et al., 2013), this region encompasses six gene models: *ART1* (LOC_Os12g07280), LOC_Os12g07290, LOC_Os12g07300, LOC_Os12g07310, LOC_Os12g07340, and LOC_Os12g07350.

To assess the levels of structural variation between *japonica* and *indica* across the 44.7-kb fine-mapped *Alt12.1* locus, we aligned sequences from the *japonica* rice reference genome, Nipponbare (which served as a proxy for Azucena) to a long-read, de novo assembly of the IR64 genome (Schatz et al., *in preparation*; http://schatzlab.cshl.edu/data/ir64/). A single IR64 scaffold was identified that covered >36 kb of the *Alt12.1* fine-mapped locus (44.7 kb). No major rearrangements were detected in the region, and both gene order and gene content were preserved (Fig. S2). Based on previous reports showing the major role played by *ART1* in rice Al resistance, and the extreme Al-sensitive phenotype of the *art1* mutant (Yamaji et al., 2009), we considered *ART1* to be the primary candidate gene underlying the Al resistance QTL *Alt12.1*.

2.3 | Allelic variation in *ART1*

To analyze the extent of allelic variation in the *ART1* gene, we examined both sequence and expression level polymorphisms. First, we sequenced the CDS in four rice varieties representing four major rice subpopulations: IR64 (*indica*), Azucena (*tropical japonica*), Kasalath (*aus*), and Nipponbare (*temperate japonica*)

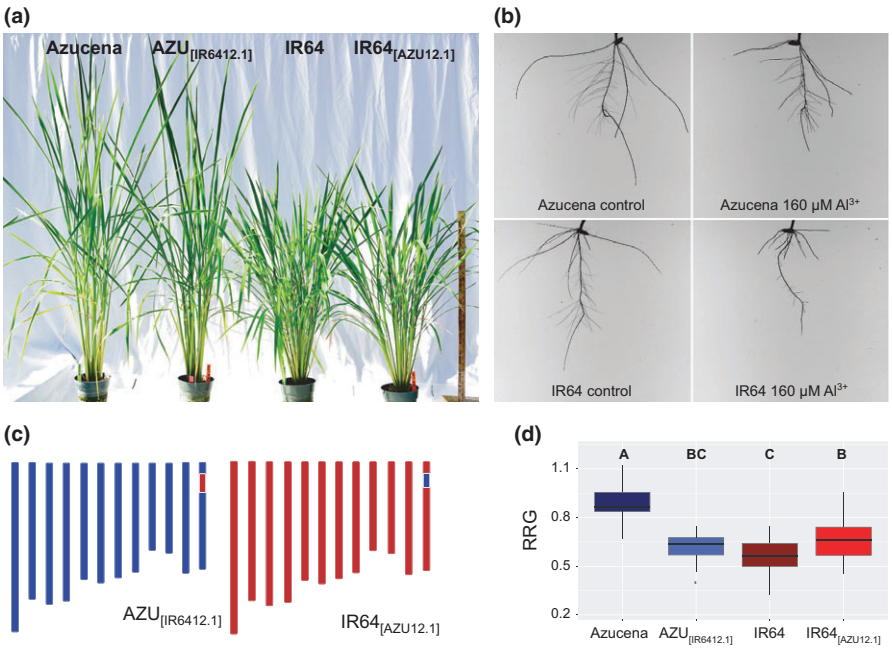

FIGURE 1 Near-isogenic lines (NILs) carrying reciprocal introgressions of the *Alt12.1* region validate the effect of the QTL on rice Al resistance. (a) Representative plants of the Al-resistant rice variety Azucena, of the Al-sensitive variety IR64, and of the reciprocal NILs near-isogenic lines $AZU_{[IR6412.1]}$ and $IR64_{[AZU12.1]}$ grown under greenhouse conditions. Photograph taken 110 days after sowing. (b) Parents of the recombinant inbred line (RIL) mapping population used to map Al resistance QTL (Famoso et al., 2011). Azucena (*tropical japonica*) is Al-resistant and IR64 (*indica*) is Al-sensitive. The photographs show roots of representative five-day-old seedlings of Azucena and IR64 grown in hydroponics under control (0 μM Al^{3+} activity, left) and Al stress (160 μM Al^{3+} activity, right) condition for five days. (c) Genotypic makeup of the near-isogenic lines $AZU_{[IR6412.1]}$ (left) and $IR64_{[AZU12.1]}$ (right). In the schematic representation of the 12 chromosomes of rice, blue denotes Azucena background, and red denotes IR64 background. The reciprocal introgressions at the *Alt12.1* region on chromosome 12 are indicated by a blue rectangle in $AZU_{[IR6412.1]}$ and by a red rectangle in $IR64_{[AZU12.1]}$. (d) Al resistance phenotypes of Azucena, IR64, and the reciprocal NILs $AZU_{[IR6412.1]}$ and $IR64_{[AZU12.1]}$. Relative root growth (RRG) was calculated as the ratio between the total root growth (TRG) of seedlings ($n = 18$) grown under stress conditions (160 μM Al^{3+} activity) over TRG of seedlings ($n = 18$) grown under control conditions (0 μM Al^{3+} activity)

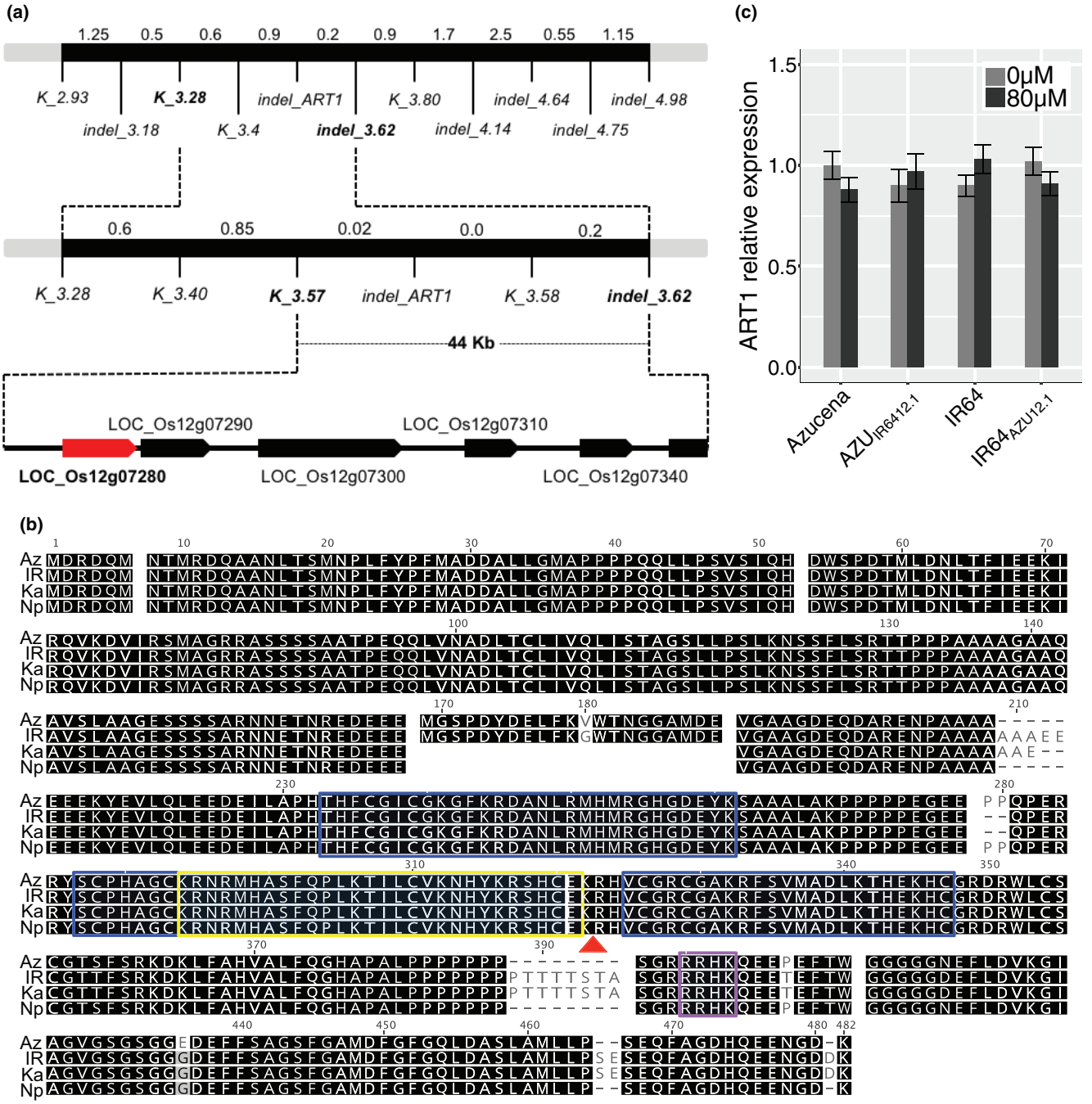

FIGURE 2 The rice Al resistance gene *AL RESISTANCE TRANSCRIPTION FACTOR 1* (*ART1*) localizes to the fine-mapped region of the Al resistance QTL *Alt12.1*. (a) Fine-mapping schema. The Al resistance QTL *Alt12.1* was fine-mapped using 4,224 F_3 and 3,552 F_4 plants from a cross between the Al-sensitive parent IR64 and an Al-resistant recombinant inbred line from the Azucena × IR64 mapping population (Appendix S2). The black bar represents a region of rice chromosome 12; molecular markers used at each step are indicated below the bar. Genetic distances are shown in pseudo cM above the black bar (1 cM ~200,000 bp). *ART1* (LOC_Os12g07280) is highlighted (red); other genes in the region are also represented (black arrows). (b) Alignment of the predicted ART1 amino acid sequences from Azucena, IR64, Kasalath, and Nipponbare. Predicted C2H2 domains (blue box) are shown; predicted monopartite (purple rectangle) and bipartite (yellow rectangle) nuclear localization domains are also shown. A red triangle under the alignment indicates the position of the 1-bp deletion found in the *art1* mutant (Yamaji et al., 2009). (c) *ART1* relative expression in rice roots, measured using RT-qPCR. Azucena, IR64, and the reciprocal NILs $AZU_{[IR6412.1]}$ and $IR64_{[AZU12.1]}$ were grown in hydroponics and treated with Al (80 μM Al^{3+} activity) for 4 hr. Control: light-gray bar; Al stress, dark-gray bar. RNA was collected from six independent biological replicates. Error bars indicate a 95% confidence interval. All pairs of means were compared using a Tukey–Kramer HSD test and no significant differences were found ($p < .05$)

(Garris, Tai, Coburn, Kresovich, & McCouch, 2005; Zhao et al., 2011). Azucena and Nipponbare, both Al-resistant *japonica* cultivars (Famoso et al., 2011), differ from each other by a single, nonsynonymous amino acid substitution at position 436 of the ART1 protein (Figure 2b). IR64 and Kasalath, both Al-sensitive cultivars, differ from each other by one nonsynonymous substitution (position 53) and two indels (positions 168 and 210–211). The two *japonica* cultivars differ from the *indica* and *aus* cultivars by a total of 11 polymorphisms (4 aa substitutions and 7 indels). The most notable difference is a large C-terminal insertion (8 aa) that is present in IR64 and Kasalath (position 387–395) but absent in Azucena and Nipponbare. Between Azucena and IR64, the parents of the mapping population used in this study, we observed 4 aa substitutions and 7 indels (Figure 2b).

Next we examined *ART1* expression levels in Azucena, IR64, and the reciprocal NILs $AZU_{[IR6412.1]}$ and $IR64_{[AZU12.1]}$. An RT-qPCR study in the presence and absence of Al found that *ART1* expression is not responsive to Al stress in the roots of Azucena, $AZU_{[IR6412.1]}$, IR64, and $IR64_{[AZU12.1]}$, and that there are no significant differences ($p < .05$) in *ART1* transcript accumulation in the roots of any of the four lines (Figure 2c). These results suggest that the phenotypic variation associated with the *Alt12.1* QTL is likely due to genetic variation in the *ART1* coding region rather than expression level polymorphism.

2.4 | Functional analysis of the proteins encoded by different *ART1* alleles

In light of the polymorphisms observed in the *ART1* CDS, we were interested to determine whether the proteins encoded by the different *ART1* alleles differ in their nuclear targeting and/or DNA-binding affinity. *In silico* analysis of the predicted ART1 proteins identified a bipartite nuclear localization signal upstream of the functional 1-bp frameshift mutation reported by Yamaji et al. (2009) in the *art1* mutant (Figure 2b). This differed from the monopartite nuclear localization domain originally reported by Yamaji et al. (2009), which occurred downstream of the frameshift mutation. We used YFP fusions to determine the subcellular localization of the proteins encoded by the four natural *ART1* alleles as well as the aberrant protein expressed by the *art1* mutant. The *art1* mutant is characterized by a single-nucleotide deletion that disrupts the frame of translation at position 317, resulting in a longer protein (477 amino acids; the wild-type ART1 is 465 amino acids). The *art1* mutant version was generated via mutagenesis in vitro (see Materials & Methods). C-terminal YFP fusion proteins were expressed in tobacco leaves under control of a 35S promoter. A strong YFP signal was detected in the nucleus of cells of tobacco leaves expressing all four ART1 alleles as well as the *art1* mutant (Figure 3a). We conclude that the polymorphisms in the *ART1* coding region do not affect the subcellular localization of the protein.

Next we compared the DNA-binding ability of the proteins encoded by different *ART1* alleles in yeast one-hybrid assays (Figure 3b). To evaluate the DNA-binding ability of the Nipponbare, Azucena, Kasalath, IR64, and *art1*-mutant alleles, we used stably transformed yeast lines carrying a fragment of the *OsSTAR1* promoter known to contain the ART1 binding site and previously used in yeast one-hybrid assays (Yamaji et al., 2009) to drive a beta-galactosidase reporter gene (Figure 3b). When quantified via β-galactosidase assays, the *art1* mutant allele was unable to activate the reporter (Figure 3c), in agreement with the fact that the 1-bp frameshift mutation in the *art1* mutant disrupts one of the predicted DNA-binding domains. The *japonica* alleles found in Nipponbare and Azucena, which differed by a single amino acid, showed comparable levels of reporter gene activation, indicating that they have similar DNA-binding affinity (Figure 3c). The *aus* allele from Kasalath and the *indica* allele from IR64 activated the reporter gene at similar levels. On the other hand, the two *japonica* alleles (Azucena and Nipponbare) activated the reported gene at significantly lower levels ($p < .05$) when compared to the *indica*/*aus* alleles (IR64 and Kasalath).

2.5 | Whole-transcriptome analysis in roots of Azucena, IR64, and the reciprocal NILs

We hypothesized that the polymorphisms also affect DNA binding of the TF *in planta*, and its ability to activate downstream genes in response to Al stress. We examined this by performing transcriptome analysis in roots of Azucena, IR64, and the reciprocal NILs under Al stress using RNA-seq. Seedlings of Azucena, IR64, and the reciprocal NILs $AZU_{[IR64121]}$ and $IR64_{[AZU12.1]}$ were grown in hydroponics, then subjected to treatment with or without Al for 4 hr. Four independent biological replicates per genotype per treatment were collected and analyzed. A total of ~580M reads were generated across the 32 samples, with an average of ~18M reads per sample. After removing adaptors, low-quality sequences, and reads that align to ribosomal RNA, we uniquely mapped ~360M reads to the Nipponbare reference genome (MSUv.7), averaging 11M reads per sample (Table S3). Raw read counts for each gene model were used to identify differentially expressed genes. The genotypic identity of all samples was confirmed by visualizing SNPs both within and outside the introgression regions (Table S4). Differentially expressed genes were selected according to the following criteria: (i) twofold or greater change in transcript abundance; (ii) adjusted p value of $\leq .05$; and (iii) minimum of eight counts in at least one sample.

Samples of each reciprocal NIL were analyzed alongside samples of their respective recurrent parents, to avoid spurious results due to genotypic differences across the *indica* and *japonica* genetic backgrounds. A principal component analysis (PCA) on normalized counts was performed to determine which variance components explain most of the global transcriptional variation. In the Azucena background (Azucena and NIL $AZU_{[IR6412.1]}$), the first PC explains 44.5% of the variation and separates control from Al-treated samples (Fig. S3a). The second PC (23.7%) differentiates the two genotypes. In the IR64 background (IR64 and NIL $IR64_{[AZU12.1]}$), the first PC explains 62% of the transcriptional variation, distinguishing the Al-treated $IR64_{[AZU12.1]}$ samples from all others. The second PC (12.7%)

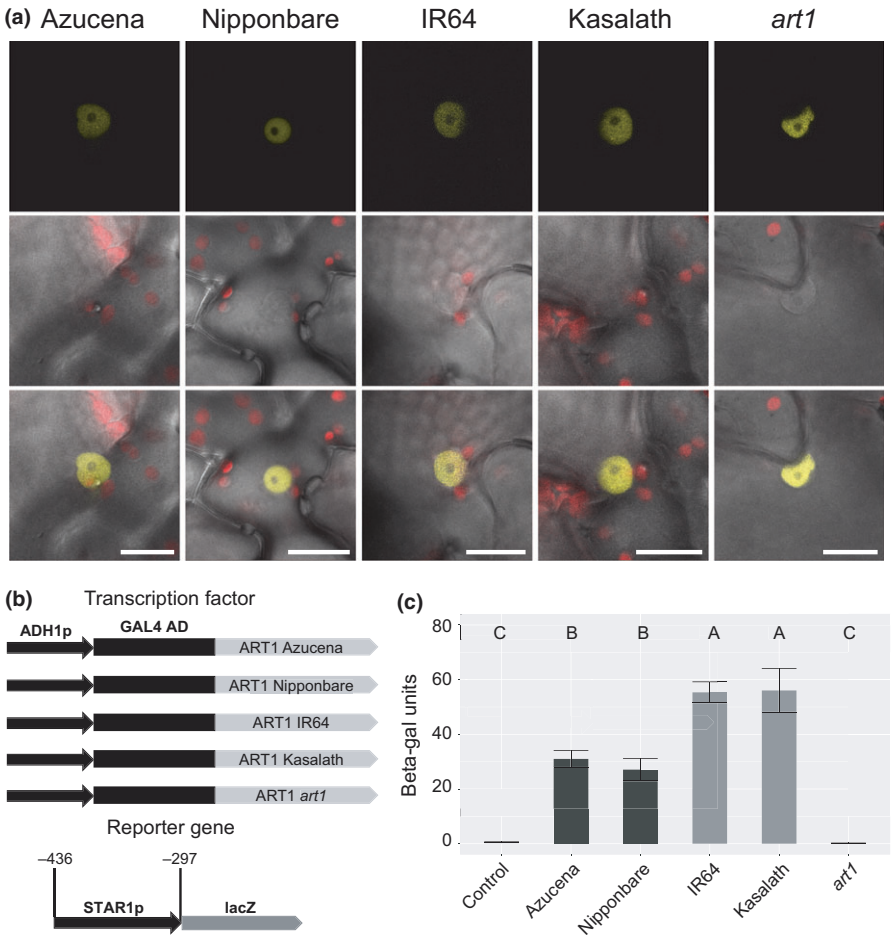

FIGURE 3 Proteins encoded by different *ART1* alleles localize to the nucleus, but differ in their DNA-binding affinity. (a) Subcellular protein localization of ART1 using C-terminal YFP gene fusions (ART1:YFP) transiently expressed in tobacco (*N. benthamiana*). Plasmids carrying the Azucena, Nipponbare, IR64, Kasalath, or *art1* mutant allele of ART1 were individually infiltrated into tobacco leaves. The top row shows the YFP fluorescence, while the middle row shows the superimposed chloroplast fluorescence and bright field channels. The third row shows merged images from all three channels (YFP fluorescence, chloroplast fluorescence, and bright field). Scale bar = 20 μm. (b) Schematic diagram of the constructs used in yeast one-hybrid assays. For the reporter construct, a fragment of the *STAR1* promoter was cloned in front of the *lacZ* gene and integrated into the yeast genome. Individual yeast colonies carrying the reporter construct were selected and transformed with one of five different transcription factor constructs. Each transcription factor construct contained the constitutive ADH1 promoter driving the expression of the GAL4 activation domain (GAL4 AD) fused to the *ART1* CDS from Azucena (*tropical japonica*; Al-resistant), Nipponbare (*temperate japonica*; Al-resistant), IR64 (*indica*; Al-sensitive), Kasalath (*aus* Al-sensitive), and the *art1* mutant allele. (c) Yeast one-hybrid assay comparing promoter activation by different *ART1* alleles. A 164-bp fragment of the *OsSTAR1* promoter was used. Constructs carrying an empty vector (control), or the Azucena, Nipponbare, IR64, Kasalath, or *art1* mutant allele were assayed for beta-galactosidase reporter gene activity (n = 10). Error bars indicate standard deviation. All pairs of means in (c) were compared using a Tukey–Kramer HSD test; lines not connected by the same letter are significantly different ($p < .05$)

separates the Al-treated IR64 samples from the control samples (Fig. S3b). In both genetic backgrounds, the main source of transcriptional variation was Al treatment. However, in the IR64 background, the effect of Al treatment was more accentuated in the NIL $IR64_{[AZU12.1]}$.

A total of 495 unique genes showed differential expression in response to Al across the four genotypes under study: 215 genes were up-regulated and 280 were down-regulated (Figure 4). The parental lines Azucena (*tropical japonica*, Al-resistant) and IR64 (*indica*, Al-sensitive) showed similar numbers of up-regulated genes (Azucena = 98; IR64 = 81), and half of them were shared across the two genotypes (n = 40; Figure 4b). In contrast, Azucena showed a larger number of genes that were down-regulated in response to Al stress (n = 148) compared to IR64 (n = 35), and only 16 of them were shared.

2.6 | The effect of the reciprocal *Alt12.1* QTL introgressions on gene expression

We first examined the RNA-seq results for each NIL alongside its recurrent parent grown under control conditions (absence of Al). When the NIL $AZU_{[IR6412.1]}$ was compared to its recurrent parent Azucena, 62 differentially expressed genes were detected (File S2). Of these, 40 are located within the introgression from IR64 in

$AZU_{[IR6412.1]}$, and are interpreted to represent genotypic differences between *indica* and *japonica*. Three of them were also found to be differentially regulated by Al in Azucena: two were down- and one was up-regulated (File S2). When the NIL $IR64_{[AZU12.1]}$ was compared to IR64 under control conditions, 14 differentially expressed genes were identified. Seven of them are located within the 2.36-Mb introgression from Azucena in $IR64_{[AZU12.1]}$. Of these 14 genes, two were up-regulated by Al in IR64 (File S2). None of the differentially expressed genes detected under control conditions corresponds to genes reported in previous studies to be Al-responsive (Arenhart et al., 2014; Tsutsui et al., 2012; Yamaji et al., 2009).

One gene, LOC_Os12g07340, located within the 44-kb fine-mapped region of the *Alt12.1* QTL, was differentially expressed in both Azucena and IR64 backgrounds. According to RNA-seq, LOC_Os12g07340 expression is higher in Azucena than in the NIL $AZU_{[IR6412.1]}$ (Fig. S4a) and also higher in the NIL $IR64_{[AZU12.1]}$ than in IR64. This suggests that the Azucena allele is more highly expressed than the IR64 allele. Under Al stress, LOC_Os12g07340 is down-regulated by Al in lines carrying the Azucena allele, although the difference is only significant in Azucena (Fig. S4b). LOC_Os12g07340 encodes an expressed protein with no known functional domains; whether this gene also contributes to the Al resistance phenotype associated with the *Alt12.1* QTL merits further investigation.

2.7 | The effect of the *Alt12.1* QTL introgressions on the transcriptional response to Al stress

While our RNA-seq data showed that the reciprocal *Alt12.1* introgressions triggered few changes in gene expression in the absence of Al, significant changes were observed in response to Al stress. In the Azucena genetic background, the presence of the *ART1* allele from IR64 reduced the number of up-regulated genes in the NIL $AZU_{[IR6412.1]}$ (n = 71) relative to Azucena (n = 98). Of these, 54 were shared between Azucena and the NIL (Figure 4b). In contrast, in the IR64 genetic background, the presence of the *ART1* allele from Azucena did not greatly affect the number of up-regulated genes (n = 81 in IR64 versus n = 86 in the NIL $IR64_{[AZU12.1]}$), and 38 of these were shared between the two genotypes (Figure 4b).

The down-regulation of genes in response to Al stress showed a distinct pattern: 148 genes were down-regulated in Azucena, while only 36 were down-regulated in the NIL $AZU_{[IR6412.1]}$ (Figure 4). Conversely, 35 genes were down-regulated in IR64 and 165 in the NIL $IR64_{[AZU12.1]}$. In other words, genotypes carrying the *ART1* allele from Al-resistant Azucena showed a greater number of down-regulated genes than those carrying the IR64 *ART1* allele. Of the 148 genes down-regulated in Azucena and 165 down-regulated in the NIL $IR64_{[AZU12.1]}$, only 45 are in common. A GO analysis showed that the down-regulated genes in all four genotypes were strongly enriched in the categories "response to stimulus" and "primary metabolic processes" (File S3). Azucena and both NILs were also enriched for genes involved in "signal transduction" and "developmental processes," but this was not true for IR64. The GO analysis suggests that the larger number of down-regulated genes in genotypes carrying the Azucena *ART1* allele encompasses a number of different functional categories (Fig. S5).

A comparison of global transcriptional responses between each NIL and its parent indicated that the reciprocal *Alt12.1* introgressions influenced the magnitude of the transcriptional response to Al. The average fold-change across all up-regulated genes was significantly lower in the NIL $AZU_{[IR6412.1]}$ than in Azucena (Figure 5a,c). The same was true for down-regulated genes, which were significantly less down-regulated in the NIL $AZU_{[IR6412.1]}$ than in the parent. Conversely, the NIL $IR64_{[AZU12.1]}$ showed greater fold-changes in both up- and down-regulated genes than IR64 (Figure 5b,d). These results suggest that genes in both genetic backgrounds are transcriptionally more responsive to the *ART1* allele from Al-resistant Azucena.

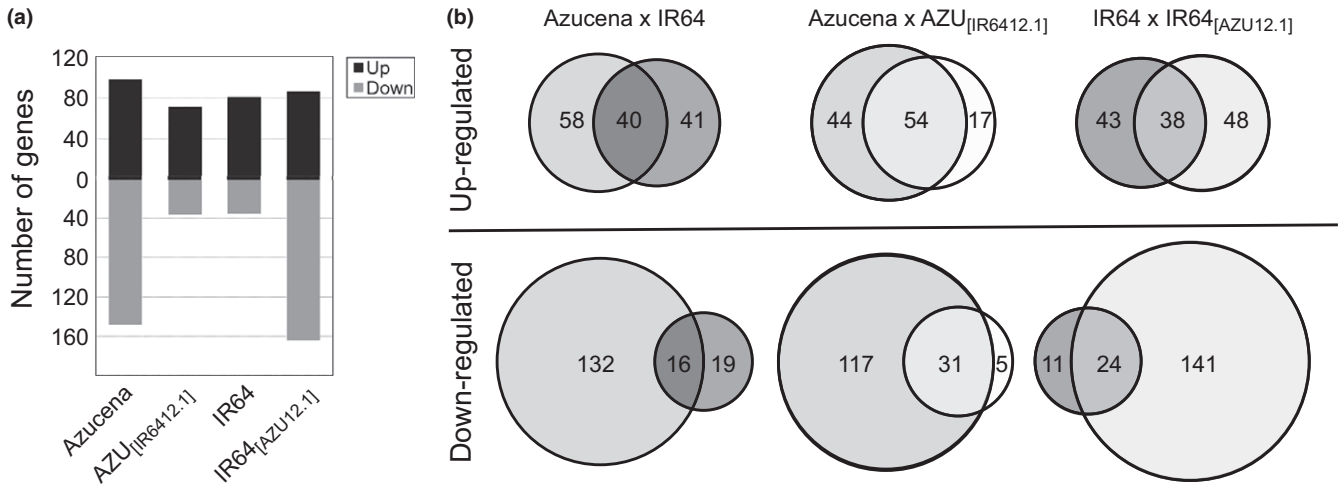

FIGURE 4 Azucena, IR64, and the reciprocal NILs $AZU_{[IR6412.1]}$ and $IR64_{[AZU12.1]}$ differ in their gene expression responses to Al stress. (a) Bar plot displaying the number of differentially regulated genes in response to Al in roots of Azucena, IR64, and the reciprocal NILs $AZU_{[IR6412.1]}$ and $IR64_{[AZU12.1]}$ according to RNA-seq. Plants were treated with 0 or 80 μM Al^{3+} activity for 4 hr. (b) Venn diagrams of differentially regulated genes in response to Al in each genotype

Next, we identified specific genes displaying higher fold-change in response to Al in the lines carrying the Azucena *ART1* allele (Figure 6). The heat map in Figure 6a displays differentially regulated genes in Azucena background, sorted according to the difference in fold-change in Azucena (native Azucena *ART1* allele) relative to the NIL carrying the IR64 *ART1* allele. Among those up-regulated by Al, 26 genes were >1.5-fold more up-regulated in Azucena than in $AZU_{[IR6412.1]}$. Of these genes, 12 were more than twofold more up-regulated in Azucena than in the NIL $AZU_{[IR6412.1]}$ (Table 1 and File S4). These genes are at the top of the heat map (Figure 6a). A similar pattern was observed for down-regulated genes. There were no genes displaying the opposite behavior; in other words, all differentially regulated genes were either similarly or more intensely regulated in Azucena than in the NIL carrying the IR64 allele of *ART1*.

In the IR64 background (Figure 6b), genes were sorted according to the difference in fold-change in the NIL $IR64_{[AZU12.1]}$ (*ART1* allele from Azucena) relative to IR64, so that genes that respond more strongly in the presence of *ART1* from Azucena are at the top of the heat maps. Among the up-regulated genes, 32 genes were >1.5-fold more up-regulated in $IR64_{[AZU12.1]}$ than in IR64. Of these, ten were more than twofold more up-regulated in $IR64_{[AZU12.1]}$ than in IR64 (Table 2 and File S4). A number of genes were more up-regulated in IR64 than in the NIL $IR64_{[AZU12.1]}$ (File S4; bottom of heat map in Figure 6b). The biological basis for this is not known; a possible explanation may be that IR64, being less Al-resistant, is under more stress, and therefore, more stress-related genes are differentially regulated.

Next, we examined whether the genes responding differently to the Azucena versus the IR64 *ART1* allele were the same or different in the two genetic backgrounds. A total of 26 genes showed greater up-regulation by the Azucena *ART1* allele in the Azucena background, while 32 showed greater up-regulation by the Azucena *ART1* allele in the IR64 background. Only six were shared across the two (Fig. S6a). A total of 48 genes showed greater down-regulation by the Azucena *ART1* allele in the Azucena background, while 95 showed greater down-regulation by the Azucena *ART1* allele in the IR64 background. Only eight were shared (Fig. S6a). Although only two genotypes were tested, these results suggest that the genetic background influences the ART1-mediated transcriptional responses to Al stress. These results also indicate that many Al-responsive genes are independent of the *ART1* allele, or independent of ART1 altogether.

2.8 | Functional annotation of genes that respond more to Al stress in the presence of the Azucena *ART1* allele

In previous mutant studies, 32 genes were reported to be up-regulated by Al stress in wild type but not in the *art1* mutant (Yamaji et al., 2009; Yokosho, Yamaji, & Ma, 2011); these 32 genes have been designated ART1-regulated genes. Several of these were also identified in our study. The parental lines Azucena (Al-resistant) and IR64 (Al-sensitive) up-regulated 17 and 10 "ART1-regulated" genes,

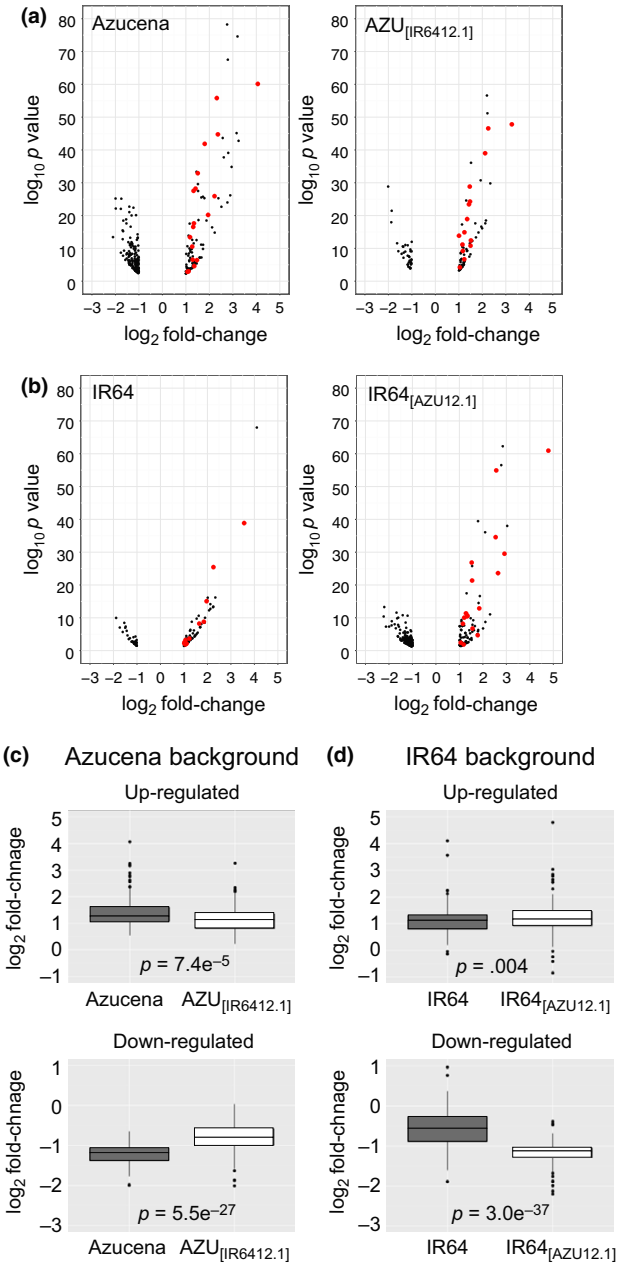

FIGURE 5 Gene expression responses to Al stress differ in magnitude in Azucena (*tropical japonica*) and IR64 (*indica*) genetic backgrounds. (a) and (b): Volcano plots showing gene expression responses to Al stress in each genotype. The ($-\log_{10}$-transformed) *p* values were plotted against $\log_2$ fold-change for each differentially regulated gene. (a) Azucena background; (b) IR64 background. Genes described by Yamaji et al. (2009) are highlighted in red. (c) and (d): boxplots of gene expression changes ($\log_2$ fold-change) of genes in Azucena (c) and IR64 (d) backgrounds. Genes up-regulated in Azucena in response to Al (n = 98) are significantly more up-regulated than those in the NIL $AZU_{[IR6412.1]}$ (n = 71) (p value = 7.4e-05). Genes down-regulated in Azucena (n = 148) are significantly more down-regulated than those in the NIL $AZU_{[IR6412.1]}$ (n = 36) (p value = 5.55e-27). Conversely, genes in IR64 (n = 81) are less up-regulated in response to Al than those in the NIL $IR64_{[AZU12.1]}$ (n = 115) (p value = .004). Genes down-regulated in IR64 (n = 35) are significantly less down-regulated than those in the NIL $IR64_{[AZU12.1]}$ (p value = 3e-37) (n = 164)

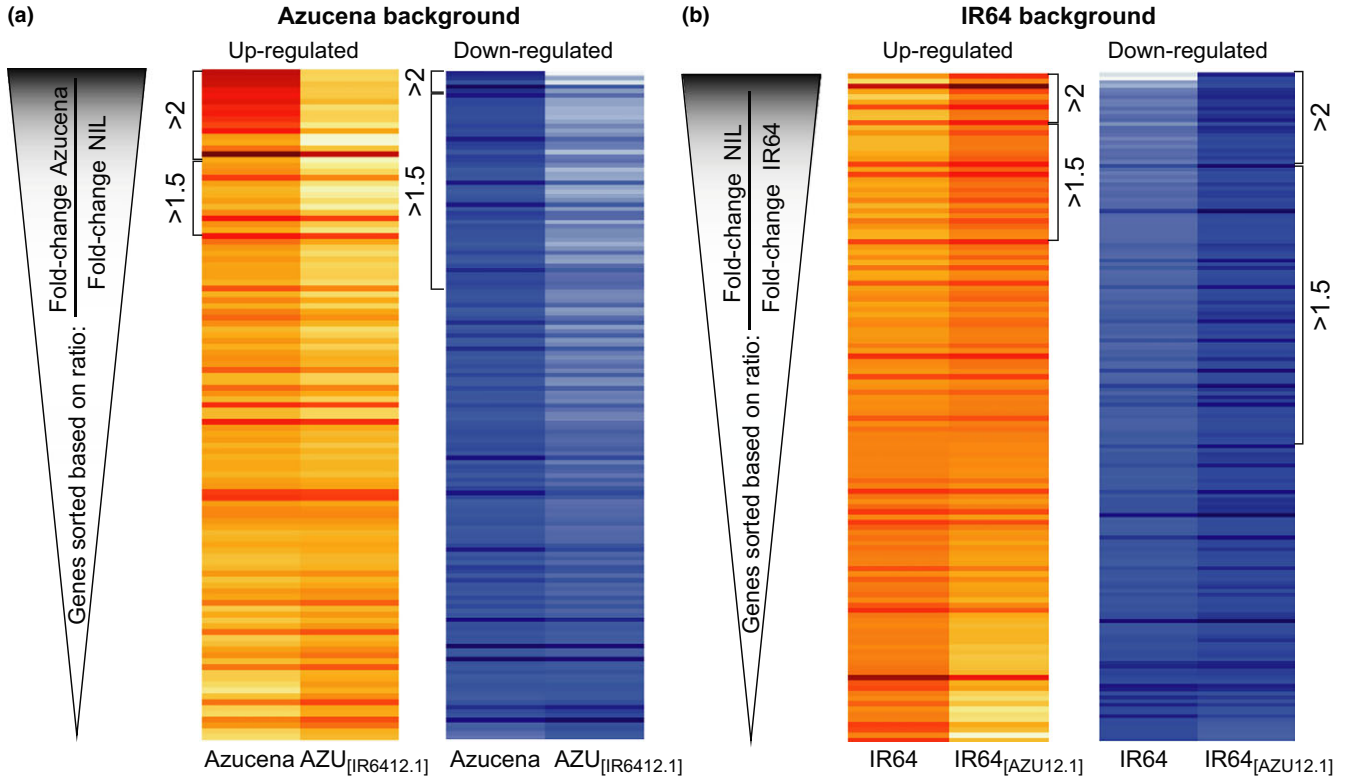

FIGURE 6 Differential gene expression responses to Al stress are stronger in the presence of the ART1 allele from Azucena in both genetic backgrounds. Heat maps illustrating the RNA-seq expression profile (log_2 fold-change) of differentially regulated genes in response to Al in (a) Azucena and (b) IR64 backgrounds. Genes were sorted according to the ratio between the fold-change (in response to Al) in the line carrying the Azucena ART1 allele and the line carrying the IR64 ART1 allele. In other words, Azucena background lines were sorted based on fold-change in Azucena/fold-change in NIL $AZU_{[IR6412.1]}$. In the case of IR64 background, lines were sorted based on fold-change in $IR64_{[AZU12.1]}$/fold-change in IR64. Brackets in (a) indicate genes with (fold-change Azucena/fold-change NIL $AZU_{[IR6412.1]}$) ratios above 2 and above 1.5. Brackets in (b) indicate genes with (fold-change in $IR64_{[AZU12.1]}$/fold-change in IR64) ratios above 2 and above 1.5. The color key represents normalized, log_2-transformed fold-change. For up-regulated genes, red indicates high fold-change and light yellow indicates low (or no) fold-change. For down-regulated genes, dark blue indicates high fold-change and light blue indicates low (or no) fold-change

respectively (Figure 5). Of these, eight were shared across the two genotypes (Fig. S6b). The NIL $AZU_{[IR6412.1]}$ up-regulated 14 genes; of these, 13 were shared between Azucena and the NIL. In the IR64 genetic background, the NIL $IR64_{[AZU12.1]}$ up-regulated 17 "ART1-regulated" genes while IR64 up-regulated 10, all of which were also up-regulated in the NIL.

The genes that respond more strongly to the *ART1* allele from Azucena are presumably the drivers of the phenotypic difference in Al resistance observed between NILs and their corresponding parents. Of the 26 genes more up-regulated in Azucena than in $AZU_{[IR6412.1]}$, only three were previously identified as ART1-regulated genes (File S4). Of the 32 genes that were more up-regulated in $IR64_{[AZU12.1]}$ than in IR64, seven were previously listed as ART1-regulated (File S4). These results suggest that in response to Al, ART1 regulates the expression of more genes than previously thought.

The previously described ART1-regulated gene *OsFRDL4* was more strongly up-regulated in the presence of the Azucena *ART1* allele than the IR64 allele in both Azucena and IR64 backgrounds (File S4). *OsFRDL4* encodes a MATE family transporter that mediates Al-activated citrate exudation from rice roots (Yokosho et al., 2011). In our RNA-seq study, the expression of *OsFRDL4* is affected by the presence of different *ART1* alleles, with the Azucena *ART1* allele driving greater up-regulation under Al stress than the IR64 allele. Specifically, the expression of *OsFRDL4* is more up-regulated in response to Al in the NIL $IR64_{[AZU12.1]}$ than in its recurrent parent IR64, and less up-regulated in response to Al in the NIL $AZU_{[IR6412.1]}$ than in Azucena (Fig. S7, File S4). Variation in *OsFRDL4* expression was previously associated with the presence of a 1.2-kb insertion in the promoter (Yokosho et al., 2016). This insertion is present in Azucena and absent in IR64 (Fig. S7), suggesting that, in the genetic backgrounds used our study, variation in both the ART1 protein and the *cis*-regulatory region of *OsFRDL4* may contribute to the regulation of *OsFRDL4* expression in response to Al (Fig. S7).

2.9 | ART1 *cis* element analysis

The *cis* element binding site of ART1 has been experimentally defined as the short, degenerate sequence motif GGN(T/g/a/C)V(C/A/g)S(C/G). This motif was identified based on protein gel-shift assays using the promoter of *STAR1* (Tsutsui et al., 2011). We set out to determine whether the putative regulatory regions of the Al-

TABLE 1 Genes up-regulated by Al stress showing fold-change 2 × or higher in Azucena compared to NIL $AZU_{[IR6412.1]}$

Gene	log_2FC Azucena	log2FC NIL $AZU_{[IR6412.1]}$	Annotation (MSUv7)
LOC_Os12g38270	3.25	0.79	Metallothionein, putative, expressed
LOC_Os10g38340	3.20	0.74	Glutathione S-transferase GSTU6, putative, expressed
LOC_Os03g16030	3.16	0.90	hsp20/alpha crystallin family protein, putative, expressed
LOC_Os01g43750	2.89	0.85	Cytochrome P450 72A1, putative, expressed
LOC_Os08g05960	2.80	0.86	Expressed protein
LOC_Os08g05970	2.95	1.02	Expressed protein
ChrSy.fgenesh.gene.47	2.51	0.65	Expressed protein
LOC_Os03g16020	2.62	0.79	hsp20/alpha crystallin family protein, putative, expressed
LOC_Os01g43774	2.38	0.78	Cytochrome P450 72A1, putative, expressed
LOC_Os04g27060	2.12	0.53	Oxidoreductase, aldo/keto reductase family protein, putative, expressed
LOC_Os12g38290	2.77	1.20	Metallothionein, putative, expressed
LOC_Os08g05980	1.30	0.26	Expressed protein

TABLE 2 Genes up-regulated by Al stress showing fold-change 2 × or higher in the NIL $IR64_{[AZU12.1]}$ compared to IR64

Gene	log_2FC IR64	log_2FC NIL $IR64_{[AZU12.1]}$	Annotation (MSUv7)
LOC_Os06g19130	0.88	2.31	Cadmium tolerance factor, putative, expressed[a]
LOC_Os05g11320	−0.13	1.16	Metallothionein-like protein 3B, putative, expressed
LOC_Os01g69010	3.56	4.79	MATE efflux protein, putative, expressed (FRDL4)[b]
LOC_Os04g01690	0.65	1.87	Pyridoxal-dependent decarboxylase protein, putative, expressed
LOC_Os05g33900	−0.04	1.09	Auxin-induced protein 5NG4, putative, expressed
LOC_Os12g38290	0.58	1.66	Metallothionein, putative, expressed
LOC_Os04g41750	1.85	2.92	Expressed protein[b]
LOC_Os11g41840	0.27	1.28	Transporter family protein, putative, expressed
LOC_Os06g39700	0.21	1.21	DNA-directed RNA polymerase subunit alpha, putative, expressed
LOC_Os02g09390	1.65	2.65	Cytochrome P450, putative, expressed[b]

[a]Gene annotation not confirmed by BlastP (see File S4).
[b]Gene also listed by Yamaji et al. (2009).

regulated genes in our whole-transcriptome analysis are enriched for the ART1-binding motif. As the first step, we probed the prevalence of the motif in the background, that is, throughout the putative regulatory regions of all rice genes, regardless of their expression pattern. We generated a library of putative regulatory regions for all rice gene models based on the rice reference genome assembly (MSUv.7), defined as the 2-kb region upstream of the start codon of each gene. When the ART1 *cis*-acting element GGNVS was mapped to the library of putative regulatory regions, the element was found to be present in 55,552 of 55,554 putative regulatory sequences, with an average of 30.3 motifs per 2-kb sequence (Fig. S8a). Because ART1 was shown to bind with lesser affinity when certain bases were found in positions 3 and 4 of the motif (Tsutsui et al., 2011), we also mapped the less degenerate motif GGYMS, in which the bases predicted to have less affinity to ART1 were excluded. The motif GGYMS was found in 55,460 of 55,554 putative regulatory sequences, with an average of 10 hits per sequence (Fig. S8b). We determined that enrichment of the 5-bp ART1-binding *cis* element in the regulatory region of putative Al response genes is insufficient criteria for identifying ART1-regulated genes, due to the widespread presence of the motif in the background of putative regulatory regions.

2.10 | Putative ART1-regulated genes provide insight into transgressive segregation for Al resistance in rice

We identified a number of genes that responded to Al stress only in the IR64 (Al-sensitive parent) genetic background, including two previously identified as ART1-regulated genes by Yamaji et al. (2009): LOC_Os01g53090 and LOC_Os04g41750. In our RNA-seq dataset, these genes were significantly up-regulated in response to Al stress in both IR64 and the NIL $IR64_{[AZU12.1]}$ but not in Azucena or $AZU_{[IR6412.1]}$ (Figure 7a). In other words, these two genes were up-regulated only in the IR64 genetic background and not in the Azucena genetic background, and the up-regulation is triggered by either of the *ART1* alleles. We hypothesized that IR64, the Al-sensitive parent, carries positive alleles conferring enhanced Al resistance at both of these loci (and possibly others). In line with this hypothesis, we previously reported transgressive segregation for rice Al resistance (Famoso et al., 2011).

To further explore this hypothesis, we investigated the expression patterns of LOC_Os01g53090 and LOC_Os04g41750 in a line (RIL-62) from the RIL population that carries IR64 alleles at both of

these ART1-regulated loci; this RIL also carries favorable alleles from Azucena at all three previously reported Al resistance QTL (*Alt1.1*, *Alt9.1*, and *Alt12.1*, i.e., *ART1*) (Famoso et al., 2011), and shows transgressive variation for Al resistance (Figure 7b). As controls, we selected three additional RILs carrying Azucena (resistant) alleles at the three QTL, as well as at the two ART1-regulated loci: RIL-19, RIL-125, and RIL-172 (Figure 7b). Using qRT-PCR, we confirmed the observations from RNA-seq showing that both genes were strongly up-regulated in response to Al in IR64 and $IR64_{[AZU12.1]}$ but not in Azucena or $AZU_{[IR6412.1]}$. Both genes were also strongly up-regulated by Al in the transgressive RIL-62, but not in any of the control RILs (Figure 7c,d).

It is possible that variation in the *cis*-regulatory regions of these "background" genes may contribute to the difference in gene expression patterns. In fact, in the upstream regulatory region of LOC_Os01g53090, there is a "TA" repeat region just 97 bp upstream of the start codon. An alignment between the Nipponbare reference genome and the IR64 assembly showed that the repetitive region is 32 bp longer in Nipponbare (Figure 7e). LOC_Os04g41750 is not only up-regulated exclusively in the IR64 background, but also responds more strongly to Al in the presence of the ART1 from Azucena: the up-regulation of LOC_Os04g41750 in response to Al in the NIL $IR64_{[AZU12.1]}$ is higher than in IR64 (Table 2 and Figure 7). These results may illustrate how recombination between divergent parents can bring together favorable genetic variation at interacting loci that contribute to transgressive phenotypic variation in the offspring.

3 | DISCUSSION

3.1 | Allelic variation in *ART1* affects rice Al resistance

Our present study focused on a major QTL for Al resistance in rice, *Alt12.1*. This QTL was identified in an RIL mapping population derived from a cross between an Al-resistant *tropical japonica* variety (Azucena) and an Al-sensitive *indica* variety (IR64). Via fine-mapping, we narrowed down the QTL *Alt12.1* to a region of 44 kb surrounding *ART1* (Figure 2). *ART1* encodes a C2H2 transcription factor required for rice Al resistance, and regulates the expression of other known Al resistance genes. While we did not observe differences in *ART1* transcript levels between Azucena, IR64, or the NILs (with or without Al treatment), we identified extensive sequence polymorphism in the coding region. These polymorphisms are not predicted to truncate the protein product or affect the C2H2 domain but could affect protein folding and interaction with target gene promoters. It is interesting to note that most of the polymorphisms between *indica* and *japonica ART1* alleles occur at the C-terminal end of the protein. Perhaps the most notable polymorphism is the large C-terminal insertion present in Kasalath and IR64, and absent in both Azucena and Nipponbare (Figure 2). This insertion adds a poly-threonine sequence downstream of a polyproline-like sequence. The reactive hydroxyl groups on threonine are common targets for posttranslational modifications making this an interesting polymorphism for future protein–protein interaction studies.

The RNA-seq results presented here indicate that the *ART1* allele from Azucena leads to a stronger transcriptional response to Al stress in rice roots. Using yeast one-hybrid assays, we demonstrate that the ART1 proteins encoded by the alleles found in *indica*/*aus* (IR64; Kasalath) and *japonica* (Azucena; Nipponbare) differ significantly in their DNA-binding ability. In the yeast one-hybrid assay, the ART1 proteins encoded by the IR64 and Kasalath alleles activated the reporter gene more strongly than the ones from Azucena and Nipponbare (Figure 3c). This is a nonintuitive result, given that the Azucena allele drives gene expression more strongly than the IR64 allele *in planta*. Yeast one-hybrid is a heterologous system, in which the TF of interest is fused with the strong GAL4 activation domain and the DNA sequence of interest is placed upstream of a reporter gene. As such, other elements that may affect TF activity *in planta* are missing. Further studies using promoter–reporter systems in plant protoplasts will shed more light into the transcriptional activation ability of the different ART1 proteins.

3.2 | Using reciprocal NILs to study transcriptomic responses to Al in IR64 and Azucena

We generated reciprocal NILs in which the *Alt12.1* QTL region from Azucena was introgressed into IR64, and vice versa (Figure 1). The NILs validated the effect of the QTL on Al resistance in both genetic backgrounds: the NIL in the Azucena background, $AZU_{[IR6412.1]}$, is less Al-resistant than Azucena; conversely, the NIL in the IR64 background, $IR64_{[AZU12.1]}$, is more Al-resistant than IR64. Because ART1 is a transcription factor, the phenotypic differences observed between each NIL and their respective recurrent parent are likely to result from differences in the expression of genes regulated by ART1. We took advantage of the reciprocal NILs to study how the IR64 and Azucena *ART1* alleles affect transcriptomic responses to Al stress in both genetic backgrounds.

We performed RNA-seq in roots of rice seedlings of Azucena, IR64, and the reciprocal NILs $AZU_{[IR64121]}$ and $IR64_{[AZU12.1]}$ under control conditions (no Al) or exposed to Al for 4 hr. To determine the effect of the *Alt12.1* QTL introgressions on gene expression under control conditions, we compared gene expression in each NIL and its recurrent parent in the absence of Al. Under these conditions, only a small number of differentially regulated genes were identified. The majority localized to the chromosomal introgressions in each of the NILs, suggesting that these genes represent "background" genotypic differences between *indica* and *japonica*. However, five genes showed differential expression in response to Al treatment (File S2). This included LOC_Os12g07340, which is one of six genes located within the fine-mapped region, only 28 kb away from *ART1* (Figure 2a). The function of these genes is unknown, and although none are predicted to encode a regulatory protein or TF, we cannot rule out the possibility that one or more may contribute to Al resistance. Our study illustrates some of the complexities and limitations of using NILs to molecularly

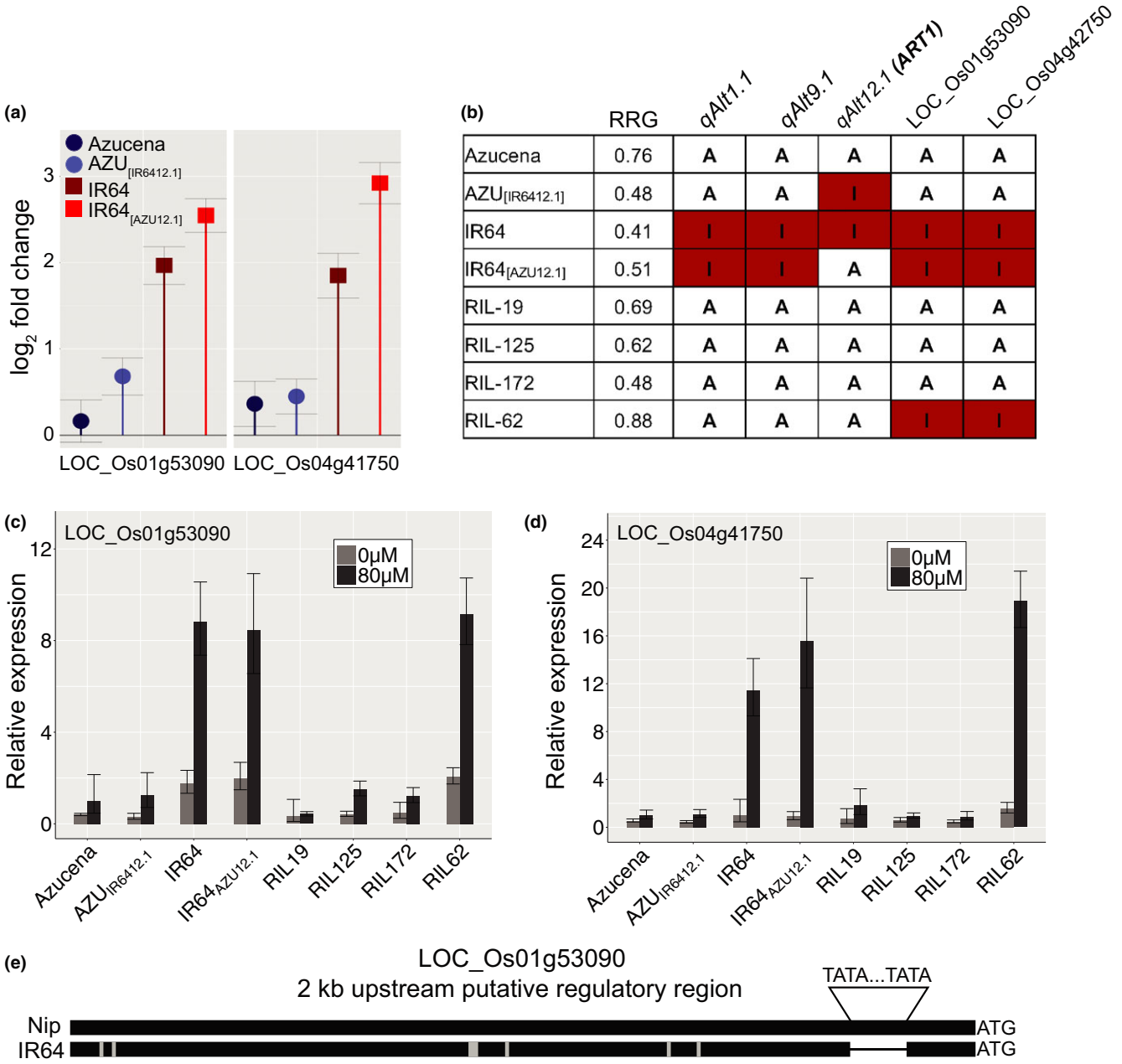

FIGURE 7 Expression patterns of ART1-regulated genes in different genetic backgrounds provide clues about transgressive variation. (a) Relative expression based on RNA-seq (log_2 fold-change) of two putative ART1-regulated genes, LOC_Os01g53090 and LOC_Os04g41750 under Al stress. (b) Genotypic makeup and Al resistance phenotype (RRG) of rice genotypes used in qRT-PCR study: the parents Azucena and IR64, the reciprocal NILs $IR64_{[AZU12.1]}$ and $AZU_{[IR6412.1]}$, and RILs 19, 125, 172 (controls), and 62. RIL-62 shows transgressive variation for Al resistance. The colored boxes indicate genotype at these loci: QTLs *Alt1.1*, *Alt9.1*, and *Alt12.1*, as well as at the putative ART1-regulated genes LOC_Os01g53090 and LOC_Os04g41750. "A" indicates Azucena genotype at that given loci; red boxes with "I" indicate IR64. (c) and (d) Relative expression based on qRT-PCR for genes (c) LOC_Os01g53090 and (d) LOC_Os04g41750 in roots of Azucena, $AZU_{[IR6412.1]}$, IR64, $IR64_{[AZU12.1]}$, RIL-19, RIL-125, RIL-172, and RIL-62 grown in hydroponics and treated for 4 hr under control (0 μM Al^{3+}) (light gray bar) and Al stress conditions (80 μM Al^{3+} activity) (dark-gray bar). Error bars indicate a 95% confidence interval. (e) Graphical representation of a DNA sequence alignment of the 2-kb putative regulatory region of LOC_Os01g53090 between the reference genome (Nipponbare) and IR64. Black bars represent regions of sequence identity. Gray rectangles indicate small indels and SNPs. A bracket indicates the position of a "TA" sequence repeat (32 bp longer in Nipponbare/Azucena relative to IR64)

characterize genes underlying QTLs. Even if the background of the NIL is clean, the target introgressions inevitably harbor more than just the gene of interest. Genome-editing tools are now well established in a variety of plant species; we are currently applying this technology to create "clean" allelic swaps for *ART1* in both *indica* and *japonica* backgrounds.

3.3 | Down-regulation of gene expression in response to Al is associated with the Azucena *ART1* allele

One of the most striking features of our RNA-seq study is the extent of the down-regulation response to Al stress in Azucena when compared to IR64 (Figure 4). Moreover, the larger number of down-regulated genes is associated with the presence of the Azucena *ART1* allele: Azucena and the IR64 NIL carrying the *Alt12.1* introgression from Azucena ($IR64_{[AZU12.1]}$) both displayed a larger number of down-regulated genes than the genotypes carrying the *ART1* allele from IR64 (IR64 and $AZU_{[IR6412.1]}$). Based on these results as well as the Y1H findings, it is tempting to speculate that ART1 may act as a negative regulator of Al responses. However, the role of ART1 as an activator of transcription is well established, as the literature provides many examples of genes involved in Al resistance in rice that are up-regulated by the stress and require ART1 for their activation. However, the possibility exists that ART1 may interact with *cis*-regulatory elements and other transcription factors to act as both an activator and a repressor of transcription.

To date, most transcriptomics studies examining responses to Al stress have focused on up-regulated genes. For instance, Yamaji et al. (2009) did not report on down-regulated genes in the *art1* mutant study, so it is not known whether the *art1* mutant also displayed less gene down-regulation in response to Al. Transcriptome studies in the Al-sensitive species *Medicago truncatula* (Chandran et al., 2008) and in the highly Al-resistant species buckwheat (Yokosho, Yamaji, & Ma, 2014) did not observe a larger number of down-regulated versus up-regulated genes. In maize, transcriptional profiling comparing an Al-resistant and an Al-sensitive genotype (Maron et al., 2008) reported that the Al-sensitive genotype showed a larger number of both up- and down-regulated genes. This is likely due to higher stress levels resulting from Al toxicity, as the number of differentially regulated genes in the Al-sensitive genotype increased over time. In our study in rice, the Al-resistant genotype displayed a larger number of down-regulated genes. However, we can only draw limited conclusions from these studies, as each study analyzed a small number of lines. More research is needed before we can implicate gene down-regulation with specific mechanisms of Al resistance.

3.4 | The effect of *ART1* on transcriptomic responses to Al stress may depend on the genetic background

Our RNA-seq study identified a number of differentially regulated genes in response to Al stress, and only about half of them were shared between the Azucena (*tropical japonica*) and IR64 (*indica*) genetic backgrounds. The ART1 from Al-resistant Azucena led to greater global changes in gene expression in response to Al stress when compared to the ART1 from IR64, in both the number of genes and magnitude of the response. This result was observed in both the Azucena (native) and the IR64 genetic background (NIL $IR64_{[AZU12.1]}$, carrying the *Alt12.1* QTL from Azucena), suggesting that the Azucena *ART1* allele is more effective in conferring Al resistance than the IR64 allele in both genetic backgrounds. The small sample size ($n = 4$ genotypes) limits our ability to statistically analyze the differences between genetic backgrounds; nevertheless, our data suggest that the identity of the genes affected by the two *ART1* alleles differed in Azucena and IR64.

3.5 | ART1 allele swapping between Azucena and IR64 affects the expression pattern of many genes not previously designated as ART1-regulated

Among the genes up-regulated by Al stress in our RNA-seq study are many previously characterized Al resistance genes, including *OsNrat1*, *OsFRDL4*, *OsFRDL2*, *OsALS1*, *STAR1*, *STAR2*, and *OsCDT3*. *OsNrat1* encodes a plasma membrane-localized Al uptake transporter (Li et al., 2014; Xia, Yamaji, Kasai, & Ma, 2010). *OsNrat1* function is likely coupled with a mechanism of internal detoxification, involving another ART1-regulated gene: *OsALS1*. This gene encodes a half-size ABC transporter localized to the tonoplast of root cells, where it is thought to sequester Al^{3+} into the vacuole (Huang, Yamaji, Chen, & Ma, 2012). *STAR1* and *STAR2* were also shown to play a role in rice Al resistance: *STAR1* encodes the nucleotide-binding domain of a bacterial-type ABC transporter that interacts with the transmembrane domain encoded by *STAR2* (Huang et al., 2009). Disruption of either gene results in higher Al sensitivity; however, the mechanism by which the STAR1-STAR2 complex confers Al resistance is unknown. When expressed in *Xenopus* oocytes, STAR1-STAR2 facilitates the export of UDP-glucose; this substrate is proposed to modify the cell wall in a way that reduces Al^{3+} accumulation. *OsCDT3* encodes a small cysteine-rich peptide that exhibits Al-binding properties (Xia, Yamaji, & Ma, 2013).

The genes that respond more strongly to the *ART1* allele from Azucena than to the *ART1* allele from IR64 are presumably the drivers of the phenotypic difference in Al resistance observed between NILs and their corresponding recurrent parents. Among the genes previously designated as ART1-regulated, only a few were among those that responded more strongly to the *ART1* allele from Azucena: *OsFRDL4*, LOC_Os02g51930 and LOC_Os02g09390 in the Azucena background, and *OsFRDL4*, LOC_Os04g41750, LOC_Os02g09390, LOC_Os11g29780, LOC_Os10g38080, LOC_Os03g55290, and LOC_Os09g30250 in the IR64 background (File S4). The functions of the vast majority of genes that responded more strongly to Al stress in the presence of the *ART1* allele from Al-resistant Azucena are unknown and present new opportunities for exploring the mechanisms of transcriptional regulation in rice roots in response to Al stress.

3.6 | Expression of the MATE transporter *OsFRDL4* is dependent on genetic background

OsFRDL4 encodes a multidrug and toxin extrusion (MATE) transporter that mediates root citrate release (Yokosho et al., 2011);

Al-activated release of organic acids from the root is a major physiological mechanism of plant Al resistance (Kochian et al., 2015). *OsFRDL4* is the major candidate for the gene underlying an Al resistance QTL in a Nipponbare (*temperate japonica*) × Kasalath (*aus*) population (Yokosho et al., 2016). The authors of that study also reported a 1.2-kb insertion in the promoter of *OsFRDL4*, and demonstrated that a majority of *japonica* varieties tested carried the insertion, while most *indica* varieties did not, and suggested that the insertion was associated with higher levels of *OsFRDL4* expression under Al stress. Yokosho et al. (2016) also concluded that the promoter of *OsFRDL4* responds equally to the ART1 proteins from Nipponbare and Kasalath. In contrast, our RNA-seq study indicates that the expression of both alleles of *OsFRDL4* is affected by the presence of the different *ART1* alleles from Azucena and IR64, with the Azucena ART1 driving greater up-regulation than the IR64 ART1. In the Azucena background, *OsFRDL4* carries the 1.2-kb insertion in the promoter (like Nipponbare), while IR64 does not (like Kasalath), and in both cases, *OsFRDL4* expression was more up-regulated by the Azucena ART1 allele than by the IR64 ART1 allele. It is possible that other regulatory elements are involved in regulating *OsFRDL4* expression in response to Al. Similarly, Melo et al. (2013) reported that sorghum NILs carrying different alleles of the major Al resistance gene *SbMATE* exhibited only partial transfer of Al resistance, which was closely correlated with a reduction in *SbMATE* expression. The authors suggest that *SbMATE* expression is regulated by multiple elements, with the relative importance of each element depending on genetic context. Our results suggest that this may also be the case for *OsFRDL4* expression in rice. Moreover, these results further illustrate the importance of genetic background, not only when selecting alleles for breeding purposes, but also when assessing gene function at the molecular level.

3.7 | ART1 *cis* element

The binding site of ART1 was experimentally defined as the short, degenerate sequence motif GGNVS, found in the promoter region of genes described as ART1-regulated. This motif was further validated for *OsSTAR1*, a known target of ART1, using EMSA (Tsutsui et al., 2011; Yokosho et al., 2011). Our results show that the presence of the *cis* element alone does not provide evidence of ART1 binding, as the short binding site is present in the promoter of almost all predicted rice genes. The very high frequency of the ART1 *cis* element in upstream regulatory regions of rice genes is not unexpected. Because the motif is both very short and very degenerate, it has a high probability of being found by chance. Evidence from the literature suggests that plant *cis* elements defined based on in vitro DNA-binding studies often contain core binding sites that are short, degenerate, and shared by multiple TFs within a transcription factor gene family (see AtcisDB: http://arabidopsis.med.ohio-state.edu/AtcisDB, and Rombauts et al., 2003). Several mechanisms control TF binding to a *cis* element only in a specific context, including sequence specificity of the TF, combinatorial cooperation between TFs, and chromatin state (Franco-Zorrilla et al., 2014; Vaahtera & Brosché, 2011; Vandepoele, Quimbaya, Casneuf, De Veylder, & Van de Peer, 2009).

It is worth noting that the list of putative ART1 targets was originally based on genes significantly mis-regulated in the *art1* mutant background. While this is a common method for defining genes regulated by a specific transcriptional activator, it can overestimate the number of true targets as TFs often regulate other TFs in complex regulatory networks. Because many TFs have low-abundance transcripts, they frequently fall below standard cutoff values in microarray and RNA-seq analyses. Thus, some of these genes may be indirectly regulated by ART1 via unidentified transcriptional regulators. Direct binding of the ART1 protein to upstream regulatory regions has only been experimentally demonstrated for *STAR1* (Tsutsui et al., 2011) and *OsFRDL4* (Yokosho et al., 2016). Furthermore, while the *art1* mutant phenotype is clearly severe, it is unclear whether it is a complete loss-of-function allele. While our own yeast one-hybrid work shows that the aberrant *art1* protein encoded by the *art1* mutant does not interact with the *OsSTAR1* promoter, our YFP fusion experiment suggests that the *art1* mutant protein does localize properly to the nucleus and contains at least one DNA-binding domain. Thus, we cannot rule out the possibility that the *art1* mutant protein disrupts the transcription of non-native ART1 targets. Nevertheless, data from our RNA-seq study of natural, functional variants suggests that ART1 has a distinct effect on transcription that is highly dependent on genetic background, and not necessarily all of the mis-regulated genes are directly regulated by ART1. Future work to validate bona fide ART1 transcriptional targets, including TF network analysis using more in-depth transcriptome data, will likely improve our functional understanding of ART1 and help to better refine its *cis*-regulatory element.

3.8 | *ART1*-regulated genes and transgressive variation for rice Al resistance

The Azucena (*tropical japonica*) X IR64 (*indica*) mapping population exhibited transgressive segregation for Al resistance (Famoso et al., 2011). This phenomenon can occur when the susceptible parent (in this case the Al-sensitive *indica* IR64) contributes positive alleles to the transgressive offspring. Using RNA-seq, we identified a number of genes that responded to Al stress only in the IR64 genetic background, including two genes previously identified as ART1-regulated by Yamaji et al. (2009): LOC_Os01g53090 and LOC_Os04g41750. The functions of these genes are not known. A BlastP search revealed LOC_Os04g41750 encodes a protein containing two DUF642 domains; DUF642 proteins constitute a highly conserved family of proteins that are associated with the cell wall and are specific to spermatophytes (Vázquez-Lobo et al., 2012). Two Arabidopsis DUF642 proteins were recently shown to regulate the activity of pectin methyl-esterase during seed germination (Zúñiga-

Sánchez, Soriano, Martínez-Barajas, Orozco-Segovia, & Gamboa-deBuen, 2014). The cell wall plays an important role in rice Al resistance, but the exact mechanism(s) are far from understood. Therefore, the molecular function of LOC_Os04g41750 is worthy of further investigation.

3.9 | ART1 function beyond Al resistance?

While a majority of genes differentially expressed between each NIL and its parent under control conditions was localized to the chromosomal introgression, a small number of them were distributed on other chromosomes. Therefore, the possibility that ART1 also regulates gene expression in the absence of Al cannot be discarded. It is important to note that expression of *ART1* itself is constitutive and is not up-regulated by Al (Figure 2c); the signaling mechanism that activates ART1 binding to the promoter of Al-responsive genes in response to Al stress has not been elucidated. In addition, it is also possible that ART1 could have additional functions beyond Al resistance. In fact, *SENSITIVE TO PROTON RHIZOTOXICITY 1* (*STOP1*), the homolog of *ART1* in *Arabidopsis thaliana*, was recently implicated as a critical checkpoint in the root developmental response to phosphate starvation (Mora-Macías et al., 2017). STOP1 also regulates low pH and Al stress responses in Arabidopsis (Iuchi et al., 2007); therefore, the authors suggest that STOP1 is likely to orchestrate root responses to multiple environmental stresses. The *art1* mutant did not show decreased root elongation when exposed to cadmium, lanthanum, zinc, or copper (Yamaji et al., 2009); however, it was not phenotyped under stresses that commonly occur together with Al as part of the acid soil syndrome, such as phosphate deficiency and iron toxicity. Plants are more likely to have evolved regulatory mechanisms that respond to multiple environmental stresses that are frequently found together in nature (Maron, Piñeros, Kochian, & McCouch, 2016). Phenotyping of the reciprocal NILs carrying the *ART1* alleles from *indica* and *japonica*, as well as the *art1* mutant, under other abiotic stresses that co-occur in acid soils will shed light into the possible functions of ART1 beyond Al resistance. It will also deepen our understanding of how a TF such as ART1 can mediate quantitative forms of stress resistance, via transcriptional regulation of an orchestra of downstream genes, each with its own potential for variation that contributes to the fine-tuning of plant response to stress.

4 | MATERIALS AND METHODS

4.1 | Plant materials and plant growth conditions

Seeds of the Al-resistant rice variety Azucena (*Oryza sativa* ssp. *tropical japonica*), of the Al-sensitive variety IR64 (*Oryza sativa* ssp. *indica*), the recombinant inbred lines RIL-241, and RIL-48 were originally obtained from the Institut de recherche pour le développement (IRD, Montpellier, France) but have been amplified in the Guterman Greenhouse at Cornell University. Experiments in hydroponic nutrient solutions under control (0 μM Al^{3+} activity), and Al stress (80 or 160 μM of Al^{3+} activity) were conducted according to Famoso et al. (2010).

4.2 | Phenotyping for Al resistance

Al resistance was phenotyped as described by Famoso et al. (2010). Individual root seedling digital images were obtained to quantify total root growth (TRG) values according to Clark et al. (2013) using the software RootReader2D (www.plantmineralnutrition.net/rr2d.php). Total root growth (TRG) values from each genotype grown under control and Al stress conditions were used to estimate relative root growth (RRG) indices as described (Famoso et al., 2010). RRG values were used for further statistical analysis.

4.3 | Genotyping

For PCR analysis total DNA was extracted from fresh leaf tissue using the Extract-N-Amp™ Plant Kit according to the manufacturer's instructions (Sigma-Aldrich, www.sigmaaldrich.com/). Plants were genotyped using InDel and SNP markers based on competitive allele-specific PCR KASP™ chemistry assays (LGC, www.lgcgroup.com/). InDel and KASP™ SNP primers were identified and designed according to Imai et al. (2013) (Table S2). InDel PCR was performed using 20 ng of DNA as template and amplified using GoTaq® Green Master Mix (Promega, www.promega.com/). Conditions for amplification and visualization of InDel markers are described in Arbelaez et al. (2015). For the KASP™ markers, 10 ng of DNA was used as template and the KASP™ Assay/Master mixes (LGC, www.lgcgroup.com/) were used to amplify the KASP™ PCR products. PCR conditions and graphical viewing of genotyped KASP™ markers were carried out as described by Imai et al. (2013). Samples were genotyped using the 6K Infinium array (Illumina, www.illumina.com/). DNA was extracted using a modified CTAB protocol described by Imai et al. (2013). The 6K Infinium arrays were performed as described by Arbelaez et al. (2015).

4.4 | Quantitative real-time PCR (RT-qPCR)

Total RNA was isolated using the QIAGEN RNeasy Mini Kit according to the manufacturer's instructions (https://www.qiagen.com). In-column digestion of genomic DNA was performed using the QIAGEN RNase-Free DNase set according to the manufacturer's instructions. Single-stranded cDNA was synthesized from total RNA using the High Capacity RNA-to-cDNA Kit (Applied Biosystems) according to the manufacturer's instructions. Quantitative real-time PCR was performed employing the relative standard curve method using Power SybrGreen Mastermix (Applied Biosystems). Gene expression was normalized against three endogenous controls. Primers used were as follows. *ART1*: 5′-CCAGCCGCTGAAGACGAT-3′ and 5′-GCAGTGGCTCCGCTTGTAGT-3′; LOC_Os01g53090: 5′-CGTGAA

CAGCCTCTTCGAG-3′ and 5′-CCATCTCCCATGTCTTGATCG-3′; LOC_Os04g41750: 5′-ACTCGTTCGCCATCAAGAC-3′ and 5′-AGTAGTCGTCCTCGTCCATC-3′. Endogenous control genes: HNR, 5′-TAAGGTCGGTATCGCCAATC-3′ and 5′-GGCAGGTTCTGCAGTG GTAT-3′; Tip41, 5′-CGCTCCAGCTCTTTGAAGATAAA-3′ and 5′-ACTCTCCCCAAAAACCATCTCA-3′; 18S, 5′-GACTACGTCCCTGC CCTTTG-3′ and 5′-TCACCGGACCATTCAATCG-3′. Three technical replicates were averaged per sample per each assay. RNA from six independent biological replicates was used to measure *ART1* expression and confirm that there are no significant differences in expression between genotypes and/or treatments. One biological replicate was used to confirm LOC_Os01g53090 and LOC_Os04g41750 in NILs and parents, and to determine expression levels in the RILs.

4.5 | Subcellular localization of ART1:YFP protein fusions

In order to determine the cellular localization of the aberrant protein generated by the *art1* mutant, we re-created the mutation in vitro. This clone was also used to generate the yeast one-hybrid construct. To generate the mutant protein, we used the reference genome sequence to identify the new stop codon in the frame-shifted protein, which extended into the 3′UTR of the *ART1* locus. We then used a series of long oligos to add the required nucleotides to the previously cloned Nipponbare allele, followed by USER-based cloning to introduce the 1-bp deletion (http://www.cbs.dtu.dk/services/PHUSER/).

ART1-YFP constructs were made in pGREEN under the control of a 35S promoter. Constructs were infiltrated into 3- to 5-week-old *N. benthamiana*. After allowing 2 to 4 days for the protein to express, leaf disks were cut from tissue adjacent to the infiltration site and used for confocal microscopy. Confocal images were collected on a Leica TCS-SP5 confocal microscope (Leica Microsystems, Exton, PA) using a 63× water immersion objective. The YFP fusion protein was visualized by excitation with an argon ion laser (512 nm), and emitted light was collected between 525 and 575 nm. Chloroplasts were excited with the blue argon laser (488 nm), and emitted light was collected from 680 to 700 nm. The YFP and chloroplast fluorescence were collected on separate channels and superimposed with a bright field image collected simultaneously with the fluorescence images. Images were processed using Leica LAS-AF software (version 2.6.0).

4.6 | Yeast one-hybrid experiments

A fragment of the *STAR1* promoter along with the five *ART1* alleles was cloned into pENTR D-TOPO (ThermoFisher, www.thermofisher.com). The *STAR1* promoter fragment (164 bp) was selected according to Yamaji et al. (2009) who showed that this fragment contains an ART1 binding site. Clone identity was confirmed by Sanger sequencing, and the pENTR-*STAR1p* construct was subcloned into pLacZi-GW (Pruneda-Paz et al., 2014) by LR recombination, according to the manufacturer's instructions (ThermoFisher). Bait strains were generated by homologous recombination of pLacZi-STAR1p into the yeast strain YM4271 according to the manufacturer's protocol (Clontech, www.clontech.com). Integration was verified by PCR. The prey vectors were generated by LR recombination of the pENTR-ART1 constructs into the yeast one-hybrid compatible plasmid pDEST22, which fuses the GAL4 activation domain to the N-terminus of the transcription factor. The bait strain was then transformed using the lithium acetate method (Gietz & Schiestl, 2007) with each of the five different pDEST22-ART1 constructs, and assayed for beta-galactosidase reporter gene activity using the liquid ONPG method described in the Clontech yeast protocol handbook (Clontech). Ten independent yeast colonies were screened for each allele. Student t tests assuming unequal variance (and $\alpha = 0.05$) were performed to determine significant differences in DNA-binding affinity.

4.7 | RNA-seq experiment and analysis

Plants were germinated in the dark in moist paper rolls for 3–4 days, and then, 40 uniform seedlings per genotype were grown in control nutrient solution for five days. Subsequently, 20 seedlings per genotype were transferred into a hydroponic solution with 80 μM of Al^{3+} activity for 4 hr before total root tissue was harvested for RNA extraction. Four independent biological replicates were performed, for a total of 32 samples (4 genotypes × 2 treatments × 4 biological replicates). Total RNA was isolated from root tissue using the QIAGEN RNeasy Mini Kit according to the manufacturer's instructions (www.qiagen.com). Strand-specific RNA-seq libraries (ssRNA-seq) were constructed by Polar Genomics, as described by Pombo et al. (2014) and Zhong et al. (2011) (http://polargenomics.com/). Barcoded libraries were multiplexed by 16× for a total of 32 samples, and sequenced in two lanes of an Illumina Hiseq2000 using the single-end reads mode (Pombo et al., 2014). Raw RNA-seq reads were processed to remove adaptor and low-quality sequences using Trimmomatic (Bolger, Lohse, & Usadel, 2014). RNA-seq reads longer than 40 bp were kept. Reads were aligned to a ribosomal RNA database (Quast et al., 2013) using Bowtie (Langmead, Trapnell, Pop, & Salzberg, 2009) and matches were discarded. The resulting, high-quality reads were aligned to the MSUv7.0 rice genome annotation (Kawahara et al., 2013) using HISAT (Kim, Langmead, & Salzberg, 2015). Following alignments, raw counts for each rice gene were derived and normalized to reads per kilobase of exon model per million mapped reads (RPKM).

4.8 | Differential expression analysis

Differentially expressed (DE) genes were identified using the DESeq2 package (Love, Huber, & Anders, 2014), https://bioconductor.org/packages/release/bioc/html/DESeq2.html). Independent filtering to remove low expression genes previous to DESeq2 analysis was performed by eliminating genes that across all samples their total sum counts is below the threshold estimated as: *overall*

normalized mean counts/number of samples to be analyzed (Bourgon, Gentleman, & Huber, 2010).

Differentially expressed genes (DEGs) were selected according to the following post hoc criteria: (i) twofold or greater change in transcript abundance, up or down, measured in log2 fold-change ratio ($\log_2$FC ≥1, or ≤−1); (ii) *p* value of ≤.05, corrected for multiple testing using a false discovery rate (FDR) criteria (Benjamini & Hochberg, 1995); and (iii) minimum of eight normalized, log-transformed counts in at least one sample (Worley et al., 2016). Regularized log-transformed counts (Love et al., 2014) estimated from DESeq2 using the true experimental design option (blind = TRUE; which accounts for different library sizes and stabilizes the variance among counts) were used to generate heat maps and for principal component analysis (PCA). For PCA, the variance across all samples for normalized, log-transformed counts was estimated using the "rowVars" function in R (https://cran.r-project.org/). Genes were ranked from the most to the least variance and the 500 genes with the highest variance across all samples were used to calculate principal components using the function "prcomp" in R (https://cran.r-project.org/), as described in Love et al. (2014). Heat maps were generated in R using the package "gplots" (http://cran.stat.nus.edu.sg/web/packages/gplots/gplots.pdf) and the function "heat map.2". Principal component analysis (PCA) was carried out using the regularized logarithm-transformed counts from DESeq2. The control samples NIL $AZU_{IR6412.1}$ rep 3, IR64 rep 4, and NIL-$IR64_{AZU12.1}$ rep 1, as well as Al-treated samples NIL-$AZU_{IR6412.1}$ rep 3, IR64 rep 3, and NIL-$IR64_{AZU12.1}$ rep 1, did not group near their respective genotype/treatment samples in the PCA analysis, and therefore were removed from the PCA shown in Fig. S3. Nevertheless, all biological replicates were used for differential gene expression analysis. GO enrichment analysis was performed using Plant MetGenMAP (http://bioinfo.bti.cornell.edu/cgi-bin/MetGenMAP/home.cgi). We applied an FDR-corrected *p* value cutoff of .01.

ACKNOWLEDGMENTS

We acknowledge the following people without whom the completion of this work would not have been possible: We are grateful to Sandy Harrington, Gen Onishi, Joseph Gage, James Jones-Rounds, Anjali T. Merchant, Yuxin Xi, Francisco Agosto-Perez, Eric Craft, and Alison Coluccio for technical and management support; and to the Institute du Recherche pour le Développement in Montpellier, France for the Azucena x IR64 RIL population; and to Karl Kremling and Christine Diepenbrock for critically reviewing a draft of the manuscript.

AUTHOR CONTRIBUTIONS

JDA, LGM, AF, TOJ, ARR, MAP, and NS performed experiments; LGM, JDA, AF, QM, and ZF analyzed data; LGM, JDA, and SRM wrote the manuscript; SRM, AF, JDA, LGM, and LVK conceived the project.

ACCESSION NUMBERS

Sequences of the *ART1* alleles for Azucena, IR64, Nipponbare, and Kasalath were submitted to GenBank (accession numbers MF093140–MF093143).

Illumina RNA-seq reads were submitted to Gene Expression Omnibus (GEO; www.ncbi.nlm.nih.gov/geo/info/seq.html) at the National Center for Biotechnology Information (NCBI; www.ncbi.nlm.nih.gov/) under the accession number GSE89494.

The de novo IR64 genome assembly is available at http://schatzlab.cshl.edu/data/ir64/.

REFERENCES

Arbelaez, J. D., Moreno, L. T., Singh, N., Tung, C. W., Maron, L. G., Ospina, Y., … McCouch, S. (2015). Development and GBS-genotyping of introgression lines (ILs) using two wild species of rice, and in a common recurrent parent, cv. Curinga. *Molecular Breeding*, *35*, 81.

Arenhart, R. A., Bai, Y., Valter de Oliveira, L. F., Bucker Neto, L., Schunemann, M., Maraschin, F. S., … Margis-Pinheiro, M. (2014). New insights into aluminum tolerance in rice: The ASR5 protein binds the *STAR1* promoter and other aluminum-responsive genes. *Molecular Plant*, *7*, 709–721.

Benjamini, Y., & Hochberg, Y. (1995). Controlling the false discovery rate - a practical and powerful approach to multiple testing. *Journal of the Royal Statistical Society Series B-Methodological*, *57*, 289–300.

Bolger, A. M., Lohse, M., & Usadel, B. (2014). Trimmomatic: A flexible trimmer for Illumina sequence data. *Bioinformatics (Oxford, England)*, *30*, 2114–2120.

Bourgon, R., Gentleman, R., & Huber, W. (2010). Independent filtering increases detection power for high-throughput experiments. *Proceedings of the National Academy of Sciences of the United States of America*, *107*, 9546–9551.

Chandran, D., Sharopova, N., Ivashuta, S., Gantt, J. S., VandenBosch, K. A., & Samac, D. A. (2008). Transcriptome profiling identified novel genes associated with aluminum toxicity, resistance and tolerance in *Medicago truncatula*. *Planta*, *228*, 151–166.

Clark, R. T., Famoso, A. N., Zhao, K., Shaff, J. E., Craft, E. J., Bustamante, C. D., … Kochian, L. V. (2013). High-throughput two-dimensional root system phenotyping platform facilitates genetic analysis of root growth and development. *Plant, Cell and Environment*, *36*, 454–466.

Famoso, A. N., Clark, R. T., Shaff, J. E., Craft, E., McCouch, S. R., & Kochian, L. V. (2010). Development of a novel aluminum tolerance phenotyping platform used for comparisons of cereal aluminum tolerance and investigations into rice aluminum tolerance mechanisms. *Plant Physiology*, *153*, 1678–1691.

Famoso, A. N., Zhao, K., Clark, R. T., Tung, C.-W., Wright, M. H., Bustamante, C., … McCouch, S. R. (2011). Genetic architecture of aluminum tolerance in rice (*Oryza sativa*) determined through genome-wide association analysis and QTL mapping. *PLoS Genetics*, *7*, e1002221.

Foy, C. D. (1988). Plant adaptation to acid, aluminum-toxic soils. *Communications in Soil Science and Plant Analysis*, *19*, 959–987.

Franco-Zorrilla, J. M., López-Vidriero, I., Carrasco, J. L., Godoy, M., Vera, P., & Solano, R. (2014). DNA-binding specificities of plant transcription factors and their potential to define target genes. *Proceedings of the National Academy of Sciences*, *111*, 2367–2372.

Garris, A. J., Tai, T. H., Coburn, J., Kresovich, S., & McCouch, S. (2005). Genetic structure and diversity in *Oryza sativa* L. *Genetics*, *169*, 1631–1638.

Gietz, R. D., & Schiestl, R. H. (2007). High-efficiency yeast transformation using the LiAc/SS carrier DNA/PEG method. *Nature Protocols*, *2*, 31–34.

Huang, C.-F., Yamaji, N., Chen, Z., & Ma, J. F. (2012). A tonoplast-localized half-size ABC transporter is required for internal detoxification of aluminum in rice. *The Plant Journal*, *69*, 857–867.

Huang, C. F., Yamaji, N., Mitani, N., Yano, M., Nagamura, Y., & Ma, J. F. (2009). A bacterial-type ABC transporter is involved in aluminum tolerance in rice. *The Plant Cell*, *21*, 655–667.

Imai, I., Kimball, J., Conway, B., Yeater, K., McCouch, S., & McClung, A. (2013). Validation of yield-enhancing quantitative trait loci from a low-yielding wild ancestor of rice. *Molecular Breeding*, *32*, 101–120.

Iuchi, S., Koyama, H., Iuchi, A., Kobayashi, Y., Kitabayashi, S., Kobayashi, Y., … Kobayashi, M. (2007). Zinc finger protein STOP1 is critical for proton tolerance in Arabidopsis and coregulates a key gene in aluminum tolerance. *Proceedings of the National Academy of Sciences*, *104*, 9900–9905.

Kawahara, Y., de la Bastide, M., Hamilton, J. P., Kanamori, H., McCombie, W. R., Ouyang, S., … Schwartz, D. C. (2013). Improvement of the *Oryza sativa* Nipponbare reference genome using next generation sequence and optical map data. *Rice*, *6*, 1–10.

Kim, D., Langmead, B., & Salzberg, S. L. (2015). HISAT: A fast spliced aligner with low memory requirements. *Nature Methods*, *12*, 357–360.

Kochian, L. V., Piñeros, M. A., Liu, J., & Magalhaes, J. V. (2015). Plant adaptation to acid soils: The molecular basis for crop aluminum resistance. *Annual Review of Plant Biology*, *66*, 571–598.

Langmead, B., Trapnell, C., Pop, M., & Salzberg, S. L. (2009). Ultrafast and memory-efficient alignment of short DNA sequences to the human genome. *Genome Biology*, *10*, R25.

Li, J.-Y., Liu, J., Dong, D., Jia, X., McCouch, S. R., & Kochian, L. V. (2014). Natural variation underlies alterations in Nramp aluminum transporter (NRAT1) expression and function that play a key role in rice aluminum tolerance. *Proceedings of the National Academy of Sciences*, *111*, 6503–6508.

Love, M. I., Huber, W., & Anders, S. (2014). Moderated estimation of fold change and dispersion for RNA-seq data with DESeq2. *Genome Biology*, *15*, 1–21.

Ma, J. F., Shen, R., Zhao, Z., Wissuwa, M., Takeuchi, Y., Ebitani, T., & Yano, M. (2002). Response of rice to Al stress and identification of quantitative trait loci for Al tolerance. *Plant and Cell Physiology*, *43*, 652–659.

Maron, L. G., Kirst, M., Mao, C., Milner, M. J., Menossi, M., & Kochian, L. V. (2008). Transcriptional profiling of aluminum toxicity and tolerance responses in maize roots. *New Phytologist*, *179*, 116–128.

Maron, L. G., Piñeros, M. A., Kochian, L. V., & McCouch, S. R. (2016). Redefining 'stress resistance genes', and why it matters. *Journal of Experimental Botany*, *67*, 5588–5591.

Melo, J. O., Lana, U. G. P., Piñeros, M. A., Alves, V. M. C., Guimarães, C. T., Liu, J., … Magalhaes, J. V. (2013). Incomplete transfer of accessory loci influencing SbMATE expression underlies genetic background effects for aluminum tolerance in sorghum. *The Plant Journal*, *73*, 276–288.

Mickelbart, M. V., Hasegawa, P. M., & Bailey-Serres, J. (2015). Genetic mechanisms of abiotic stress tolerance that translate to crop yield stability. *Nature Reviews Genetics*, *16*, 237–251.

Mora-Macías, J., Ojeda-Rivera, J. O., Gutiérrez-Alanís, D., Yong-Villalobos, L., Oropeza-Aburto, A., Raya-González, J., … Herrera-Estrella, L. (2017). Malate-dependent Fe accumulation is a critical checkpoint in the root developmental response to low phosphate. *Proceedings of the National Academy of Sciences*, *114*, E3563–E3572.

Pombo, M. A., Zheng, Y., Fernandez-Pozo, N., Dunham, D. M., Fei, Z., & Martin, G. B. (2014). Transcriptomic analysis reveals tomato genes whose expression is induced specifically during effector-triggered immunity and identifies the Epk1 protein kinase which is required for the host response to three bacterial effector proteins. *Genome Biology*, *15*, 1–16.

Pruneda-Paz, J. L., Breton, G., Nagel Dawn, H., Kang, S. E., Bonaldi, K., Doherty Colleen, J., … Kay Steve, A. (2014). A genome-scale resource for the functional characterization of arabidopsis transcription factors. *Cell Reports*, *8*, 622–632.

Quast, C., Pruesse, E., Yilmaz, P., Gerken, J., Schweer, T., Yarza, P., … Glöckner, F. O. (2013). The SILVA ribosomal RNA gene database project: Improved data processing and web-based tools. *Nucleic Acids Research*, *41*, D590–D596.

Rombauts, S., Florquin, K., Lescot, M., Marchal, K., Rouzé, P., & Van de Peer, Y. (2003). Computational approaches to identify promoters and cis-regulatory elements in plant genomes. *Plant Physiology*, *132*, 1162–1176.

Spindel, J., Wright, M., Chen, C., Cobb, J., Gage, J., Harrington, S., … McCouch, S. (2013). Bridging the genotyping gap: Using genotyping by sequencing (GBS) to add high-density SNP markers and new value to traditional bi-parental mapping and breeding populations. *Theoretical and Applied Genetics*, *126*, 2699–2716.

Tsutsui, T., Yamaji, N., & Ma, J. F. (2011). Identification of a Cis-acting element of ART1, a C2H2-type zinc-finger transcription factor for aluminum tolerance in rice. *Plant Physiology*, *156*, 925–931.

Tsutsui, T., Yamaji, N., Huang, C. F., Motoyama, R., Nagamura, Y., & Ma, J. F. (2012). Comparative genome-wide transcriptional analysis of Al-responsive genes reveals novel Al tolerance mechanisms in rice. *PLoS ONE*, *7*, e48197.

von Uexküll, H. R., & Mutert, E. (1995). Global extent, development and economic-impact of acid soils. *Plant and Soil*, *171*, 1–15.

Vaahtera, L., & Brosché, M. (2011). More than the sum of its parts – How to achieve a specific transcriptional response to abiotic stress. *Plant Science*, *180*, 421–430.

Vandepoele, K., Quimbaya, M., Casneuf, T., De Veylder, L., & Van de Peer, Y. (2009). Unraveling transcriptional control in arabidopsis using cis-regulatory elements and coexpression networks. *Plant Physiology*, *150*, 535–546.

Vázquez-Lobo, A., Roujol, D., Zuñiga-Sánchez, E., Albenne, C., Piñero, D., Buen, A. G., & Jamet, E. (2012). The highly conserved spermatophyte cell wall DUF642 protein family: Phylogeny and first evidence of interaction with cell wall polysaccharides in vitro. *Molecular Phylogenetics and Evolution*, *63*, 510–520.

Worley, J. N., Pombo, M. A., Zheng, Y., Dunham, D. M., Myers, C. R., Fei, Z., & Martin, G. B. (2016). A novel method of transcriptome interpretation reveals a quantitative suppressive effect on tomato immune signaling by two domains in a single pathogen effector protein. *BMC Genomics*, *17*, 1–13.

Xia, J., Yamaji, N., Kasai, T., & Ma, J. F. (2010). Plasma membrane-localized transporter for aluminum in rice. *Proceedings of the National Academy of Sciences of the United States of America*, *107*, 18381–18385.

Xia, J., Yamaji, N., & Ma, J. F. (2013). A plasma membrane-localized small peptide is involved in rice aluminum tolerance. *The Plant Journal*, *76*, 345–355.

Yamaji, N., Huang, C. F., Nagao, S., Yano, M., Sato, Y., Nagamura, Y., & Ma, J. F. (2009). A zinc finger transcription factor ART1 regulates multiple genes implicated in aluminum tolerance in rice. *The Plant Cell*, *21*, 3339–3349.

Yokosho, K., Yamaji, N., Kashino-Fujii, M., & Ma, J. F. (2016). Retrotransposon-mediated aluminum tolerance through enhanced expression of the citrate transporter OsFRDL4. *Plant Physiology*, *172*, 2327–2336.

Yokosho, K., Yamaji, N., & Ma, J. F. (2011). An Al-inducible MATE gene is involved in external detoxification of Al in rice. *The Plant Journal*, *68*, 1061–1069.

Yokosho, K., Yamaji, N., & Ma, J. F. (2014). Global transcriptome analysis of Al-induced genes in an Al-accumulating species, common buckwheat (*Fagopyrum esculentum* Moench). *Plant and Cell Physiology*, *55*, 2077–2091.

Zhao, K., Tung, C.-W., Eizenga, G. C., Wright, M. H., Ali, M. L., Price, A. H., ... McCouch, S. R. (2011). Genome-wide association mapping reveals a rich genetic architecture of complex traits in *Oryza sativa*. *Nature Communications*, *2*, 467.

Zhong, S., Joung, J.-G., Zheng, Y., Chen, Y.-r., Liu, B., Shao, Y., ... Giovannoni, J. J. (2011). High-throughput illumina strand-specific RNA sequencing library preparation. *Cold Spring Harbor Protocols*, *8*, 940–949.

Zúñiga-Sánchez, E., Soriano, D., Martínez-Barajas, E., Orozco-Segovia, A., & Gamboa-deBuen, A. (2014). BIIDXI, the At4g32460 DUF642 gene, is involved in pectin methyl esterase regulation during Arabidopsis thaliana seed germination and plant development. *BMC Plant Biology*, *14*, 338.

SUPPORTING INFORMATION

Additional Supporting Information may be found online in the supporting information tab for this article.

How to cite this article: Arbelaez JD, Maron LG, Jobe TO, et al. *ALUMINUM RESISTANCE TRANSCRIPTION FACTOR 1* (*ART1*) contributes to natural variation in aluminum resistance in diverse genetic backgrounds of rice (*O. sativa*). *Plant Direct*. 2017;00:1–19. https://doi.org/10.1002/pld3.14